10-MDP (10-METHACRYLOYLOXYDECYL DIHYDROGEN PHOSPHATE)-MEDIATED ADHERENCE OF RESIN COMPOSITE LUTING AGENT TO RAPID-FIRED ZIRCONIA - A FRACTURE MECHANICS APPROACH

by

Mai El Najjar

MESc/M.S.K., The University of Western Ontario, 2020

DDS, Ajman University of Science & Technology, 2009

A THESIS SUBMITTED IN PARTIAL FULFILLMENT OF

THE REQUIREMENTS FOR THE DEGREE OF

MASTER OF SCIENCE

in

THE FACULTY OF GRADUATE AND POSTDOCTORAL STUDIES

(Craniofacial Science)

THE UNIVERSITY OF BRITISH COLUMBIA

(Vancouver)

August 2022

The following individuals certify that they have read and recommend to the Faculty of Graduate and Postdoctoral Studies for acceptance, a thesis entitled:

10-MDP (10-Methacryloyloxydecyl Dihydrogen Phosphate)-Mediated Adherence of Resin Composite Luting Agent to Rapid-Fired Zirconia - a Fracture Mechanics Approach

submitted by Dr. Mai El Najjar in partial fulfillment of the requirements for

the degree of Master of Science

in Craniofacial Science

Examining Committee:

Dr. N. Dorin Ruse, Professor, Department of Oral Biological & Medical Sciences, UBC

Supervisor

Dr. Nesrine Mostafa, Assistant Professor, Department of Oral Health Sciences, UBC

Supervisory Committee Member

Dr. Tom Troczynski, Professor, Department of Materials Engineering, UBC

Supervisory Committee Member

Dr. Chris Wyatt, Professor, Department of Oral Health Sciences, UBC

Additional Examiner

Abstract

Introduction: The success of all-ceramic restorations depends on a strong and stable bond to dental hard tissues, achievable by adhesive cementation. 10-methacryloyloxydecyl dihydrogen phosphate (10-MDP) is a suitable primer for zirconia-based restorations. Adherence to zirconia imparted by 10-MDP has been investigated with shear and micro-tensile bond strength tests.

Objective: This study aimed to apply fracture mechanics methodology to investigate the effect of 10-MDP on the adherence of a resin composite luting agent (RCLA) to recently introduced rapid-fired zirconia (RFZ).

Materials & Methods: Interfacial fracture toughness (IK_{IC}) was determined with the notchless triangular (NTP) specimen K_{IC} test. Seventy-eight NTP specimens were cut and ground from RFZ blocks (Katana, Kuraray, Japan), followed by rapid firing. The samples were then cut into halves and allocated to three groups, each with a different surface preparation protocol prior to bonding: 1) Control, no treatment; 2) MDP, 5 % 10-MDP ethanol primer; 3) Silane, Bisco Bis-Silane. All samples were bonded with an RCLA (3M RelyX Veneer Cement) and stored in water at 37 °*C*. IK_{IC} was determined after 24 h and 90 d storage. The results were analyzed with an independent samples t-test (α= 0.05).

Scanning electron microscopy fractographic analysis was performed on representative fractured samples from each group.

Result: At 24 h, only the MDP group could be tested [IK_{IC} (1.34 ± 0.40) MPa·m$^{1/2}$]. Samples from the other two groups were de-bonded before testing. For the MDP group, crack propagation occurred cohesively through the RCLA. After 90 d storage, the IK_{IC} of the MDP group dropped significantly, to (0.88 ± 0.3) MPa·m$^{1/2}$.

SEM images of fractured surfaces (24 h and 90 d) showed the presence of RCLA on both halves, indicative of cohesive failure within RCLA.

Conclusion: The fracture mechanics analysis confirmed the suitability of MDP as a primer for RFZ. Even though there was a significant decrease in IK_{IC} upon storage, failure took always place cohesively in the RCLA.

Lay Summary

Zirconia is the most commonly used restorative material in computer-aided design / computer-aided manufacturing (CAD/CAM) dentistry. 10-methacryloyloxydecyl dihydrogen phosphate (10-MDP) is a primer that has been extensively used for zirconia restorations. However, no studies have investigated the suitability of the 10-MDP for the newly introduced rapid-fired zirconia materials.

In general, zirconia has gathered positive attention for its flexural strength, milling capability, and ability to resist crack propagation. However, developing a successful adhesive protocol for zirconia is still under investigation. Such a protocol may contribute to the long-term success of zirconia restorations. This work aimed to investigate the suitability of 10-MDP as a primer for rapid-fired zirconia by applying fracture mechanics methodology. The results of this study show that 10-MDP is a suitable primer for rapid-fired zirconia. Even though there was a significant decrease in bonding upon storage, failure took always place cohesively in the RCLA.

Preface

All components of the research project, including research, sample calculation, sample preparation and testing, statistical analysis, and thesis writing, were accomplished by Mai El Najjar under the guidance and supervision of my supervisor Dr. N. Dorin Ruse, UBC Faculty of Dentistry. Dr. Nesrine Mostafa, UBC Faculty of Dentistry and Dr. Tom Troczynski, UBC Department of Materials Engineering, were part of the supervisory research committee.

This in-vitro study with the involvement of no human or animal subjects and bio-hazardous materials were not used in this study, and therefore, ethical approval from the UBC Ethics Board was not required.

Table of Contents

Abstract ..... **iii**

Lay Summary ..... **v**

Preface ..... **vi**

Table of Contents ..... **vii**

List of Tables ..... **xi**

List of Figures ..... **xii**

List of Abbreviations ..... **xv**

List of Symbols ..... **xvii**

Acknowledgements ..... **xviii**

Dedication ..... **xix**

Chapter 1: Introduction **1**

1.1 Overview 1

1.1.1 Metal-Ceramic Restorations 1

1.1.2 All-Ceramic Restorations 2

1.1.2.1 Classification of Dental Ceramics 3

1.1.2.1.1 Glass-Based Ceramics 3

1.1.2.1.1.1 Predominantly Glass (Feldspathic Glass) 3

1.1.2.1.1.2 Moderately Filled Glass Ceramic 4

1.1.2.1.1.3 Highly Filled Glass Ceramic 4

1.1.2.1.2 Glass-Infiltrated Ceramics 4
1.1.2.1.3 Non-Glass-Based Ceramic (Polycrystalline Ceramic) 5

1.2 Zirconia as Dental Biomaterial 6

1.2.1 History of Zirconia materials 6

1.2.2 Microstructural Properties 6

1.2.3 Classification of Zirconia-Based Ceramics 8
1.2.3.1 Zirconia-Toughened Alumina (ZTA) 8

1.2.3.2 Magnesium Partially Stabilized Zirconia (Mg-PSZ) 9

1.2.3.3 Zirconia 3Y-TZP 9

1.2.4 Recent Advances in Zirconia Dental Materials 10
1.2.4.1 Monolithic Zirconia 10

1.2.4.2 Multilayered Monolithic Zirconia 11

1.2.5 Methods of Fabrication of Zirconia 11
1.2.5.1 In-office Vs. Lab CAD/CAM 12

1.3 Dental Bonding 14

1.3.1 Dental Adhesive Systems 14

1.3.2 Adhesion to Zirconia 16
1.3.2.1. Air Particle Abraded 18
1.3.2.2 10-MDP as Zirconia Primer 19
1.3.2.3 Resin Composite Luting Agents (RCLA) 21

1.4 Testing of Adhesion 21

1.4.1 Bond Strength Testing 21

1.4.2 Fracture Mechanics 24

1.5 Clinical significance 27

Chapter 2: Research Question and Specific Aim 28

2.1 Definitive Aims 28

2.2 Research Question 28

2.3 Research Hypothesis 28

Chapter 3: Materials and Methods 29

3.1 Materials: 29

3.1.1 KATANA™ ZIRCONIA BLOCK-STML 30

3.2.1 10-MDP 30

3.1.3 Bisco® Bis-Silane 31

3.1.4 RelyX Veneer (3M. ESPE) 33

3.2 Methods 34

3.2.1 Sample Size Calculation 34

3.1.2.1 Sample Preparation 35

3.1.2.1.1 KATANA™ ZIRCONIA BLOCK-STML 35

3.1.2.1.2 Fast Sintering Processing 38

3.1.2.1.3 Resin Composite Luting Agent 42

3.2.2 Cementation Protocols 43

3.2.4 Ageing 45

3.2.5 Determination of IK_{1C} 46

3.2.6 Scanning Electron Microscopy (SEM.) 49

3.2.7 Statistical Analysis 50

Chapter 4: Results 51

4.1 Interfacial Fracture Toughness (IK_{IC}) 51

4.2 Resin Composite Luting Agent 55

4.3 SEM Characterization 58

4.3.1 MDP Group 58

4.3.2 RelyX Veneer Resin Composite Luting Agent 59

Chapter 5: Discussion 61

Chapter 6: Conclusions 68

References 69

List of Tables

Table 1:Properties of some materials for biomedical applications (29).....9

Table 2: Classification of adhesive systems. 16

Table 3: Experimental Materials.....29

Table 4: 10-MDP Primer composition. 31

Table 5: Experimental Design 34

Table 6: Results of IK_{IC} test (Mean ± SD) in MPa·m$^{1/2}$.....51

Table 7: MDP descriptive statistics. 52

Table 8: Independent samples t-test for MDP group. 52

Table 9: Results of K_{IC} test (Mean ± SD) in MPa·m$^{1/2}$ 55

Table 10: RCLA descriptive statistics.....56

Table 11: Independent samples t-test for RCLA group. 57

List of Figures

Figure 1: Crystalline phases and transition temperatures of zirconia: (a) monoclinic, (b) tetragonal and (c) cubic (28). 7

Figure 2: Schematic drawing of stress-induced toughening mechanism of zirconia at the crack tip (31). 8

Figure 3: CAD/CAM workflow (61) 13

Figure 4: Structure of 10-MDP and its functional groups. 19

Figure 5: Structure of CQ and visible light-activated free radical generation pathways (83 20

Figure 6: Possible failure modes: (a) adhesive (interface restoration-adhesive), (b) adhesive (interface tooth-adhesive), (c) cohesive in adhesive and (d) mixed (restoration-adhesive-tooth) (90) 25

Figure 7: Possible failure modes: (a) adhesive (interface restoration-adhesive), (b) adhesive (interface tooth-adhesive), (c) cohesive in adhesive and (d) mixed (restoration-adhesive-tooth) (90) 30

Figure 8: 10-MDP AK Scientific Inc. 31

Figure 9: Bisco® Bis-Silane (Two Component) 32

Figure 10: RelyX™ Veneer (3M. ESPE) 33

Figure 11: Experimental design. 35

Figure 12: Removing milling system metal stem from the KATANA block. 35

Figure 13: KATANA block cutting in two halves. 36

Figure 14: Katana half-block cut at 60° angle using a custom jig 36

Figure 15: Isomet saw and Lapidary blade. 37

Figure 16: Prism specimen grinding and polishing. 37

Figure 17: Prism specimen dimensions and prepared NTP specimens, pre-sintered. 38

Figure 18: Zircom furnace to sinter the prism specimens. 38

Figure 19: Sintering protocol as per manufacturer's recommendations. 39

Figure 20: Sintered NTP specimen dimensions and fired specimens. 40

Figure 21: Prism specimen preparation for the cementation protocols. A: marked prism in middle and end of each specimen; B: cutting the prisms in two halves; C: Final two halves of the prism specimen. 41

Figure 22: A: RCLA being dispensed into the plastic mold; B: Light cure each end; C: removed the plastic mold and light cure each side; and D: RCLA prism specimen. 42

Figure 23: Two halves of the prism specimen marked to allow proper alignment during cementation procedure. 43

Figure 24: Alignment of each half of prism specimen in cementation jig. 43

Figure 25: Diagram showing the three groups with different surface treatment: 1) Control, no treatment; 2) MDP, 10 % 10-MDP ethanol primer and 3) Silane, Bisco Bis-Silane. All samples were bonded with an RCLA (3M RelyX Veneer Cement). 44

Figure 26: Cementation procedure.....45

Figure 27: All samples were stored in distilled water at 37 °C for 24 hours before testing. A: Control group; B: MDP, 10 % 10-MDP ethanol primer and C: Silane, Bisco Bis-Silane.....46

Figure 28: NTP specimen holder. 47

Figure 29: NTP specimen holder in mounting with spacer. 47

Figure 30: NTP specimen loaded for testing. 48

Figure 31: Failure modes of an adhesive interface. 49

Figure 32: SEM samples. 49

Figure 33: Box plots of the effect of time on IKIC.....51

Figure 34: Two groups were intact before testing for 24 h. A: Control group; B: Silane, Bisco Bis-Silane.....53

Figure 35: RCLA was seen only on one of the surfaces of failed samples.....53

Figure 36: Thin film of RCLA and the clean surface of a debonded sample.....54

Figure 37: Crack arrest for the MDP group.....54

Figure 38: Cohesive failure in RCLA for the MDP group.....55

Figure 39: Box plots of the effect of time on RCLA KIC.....56

Figure 40: SEM image of 10-MDP at 24 h. 58

Figure 41: SEM image of 10-MDP at 90 d. 58

Figure 42: SEM image: Fractured surface (24h)/RelyX resin composite luting agent.....59

Figure 43: SEM image: Fractured surface/RelyX resin composite luting agent. 59

Figure 44: SEM image: Fractured surface (90d)/RelyX resin composite luting agent.....60

List of Abbreviations

μ-SBS	Micro Shear Bond Strength
μ-TBS	Micro Tensile Bond Strength
3D	Three Dimension
3Y-TZP	3 mol% Yttria Tetragonal Zirconia Polycrystal
4Y-TZP	4 mol% Yttria Tetragonal Zirconia Polycrystal
5Y-TZP	5 mol% Yttria Tetragonal Zirconia Polycrystal
APA	Airborne Particle Abrasion
Bis-GMA	Bisphenol A - Glycidyl Methacrylate
C	Cubic
CAD/CAM	Computer-Aided Design/Computer-Aided Manufacturing
CEREC	Chairside Economical Restoration of Esthetic Ceramic
CNSR	Chevron-Notched Short Rod
CQ	Camphorquinone
CTE	Coefficient of Thermal Expansion
EDMAB	Ethyl-4-(dimethylamino)benzoate
FDP	Fixed Partial Denture
HF	Hydrofluoric Acid
ISO	International Organization for Standardization
M	Monoclinic
10-MDP	10-Methacryloyloxdecyl-dihydrogen phosphate
Mg-PSZ	Magnesium Partially Stabilized Zirconia
min	Minutes

ML(Z)	Multilayered (Zirconia)
Mol %	Mole percentage
NTP	Notchless Triangular Prism
PFM	Porcelain Fused to Metal
RCLA	Resin Composite Luting Agent
RFZ	Rapid Fired Zirconia
SBS	Shear Bond Strength
SD	Standard Deviation
SEM	Scanning Electron Microscopy
SIE	Selective Infiltration Etching
SM	Subtractive Manufacturing
SPSS	Statistical Package for the Social Science
STML	Super Translucency Multilayered Zirconia
T	Tetragonal
TBS	Tensile Bond Strength
TBS	Tribochemcial Silica Airborne Particle Abrasion
TEGDMA	Triethylene Glycol Dimethacrylate
TZP	Tetragonal Zirconia Polycrystal
UDMA	Urethane Dimethacrylate
UTML	Ultra Translucency Multilayered Zirconia
Vol%	Volume Percentage
Wt	Weight
ZTA	Zirconia Toughened Alumina

List of Symbols

α	Crack length
B	Specimen thickness
D	Specimen diameter
K_{IC}	Fracture toughness (critical stress intensity factor in Mode I loading)
n	Number of samples
P_{max}	Maximum load (N)
T	Temperature (ºC)
W	Specimen length (mm)
Y^*_{min}	Dimensionless stress intensity coefficient factor minimum
Δ	Standardized difference
M	Mean
α	Significance value

Acknowledgements

As Leonardo da Vinci said: "Learning never exhausts the mind."

Thank God for kindness, generosity, and compassion for completing my journey and achieving my dream.

Thank you to my supervisor Dr. N. Dorin Ruse, for your patience, guidance, and support. I have gained critically from your treasure of knowledge and meticulous editing. I am grateful that you took me on as a master's student and had continuous faith in me over the last three years.

Thank you to my committee members, Dr. Nesrine Mostafa Dr. Tom Troczynski. Your encouraging words and thoughtful, detailed feedback have been vital to me during my research journey.

Many thanks to my friend and classmate Dr. Ravdeep Mann for all the kind words and support you provided during our residency and research.

Thank you to the Rotsaert Dental laboratory, especially Mr. Derek Kent, laboratory technologist. He so generously took time out of his schedules to participate in my research and make this project happen.

Thank you to my friend Dr. Visalakshi Shivaraman for your support and generosity during my residency.

I would also like to thank my fellow co-residents and my Prosthodontics faculty members for their continues support and encouragement throughout journey. It has been a pleasure working with you all.

Warm thanks everyone for the help and for making this research project happen.

Dedication

Thank you to my family for your endless support. You have always stood behind me, and this was no exception. Mom, thank you for fielding a random number of calls, for calming me down and for proofreading anytime. Dad, thank you for all of your love and for constantly reminding me of the end goal.

Thank you to my sister and brothers for always being there for me and telling me that I am fantastic even when I did not feel that way.

Chapter 1: Introduction

1.1 Overview

Metal-ceramic restorations have been the most popular dental restorations for the last several decades (1). This type of restoration has gained popularity due to its superior performance and aesthetics (2). However, continuous demands for improved aesthetics and concerns related to biocompatibility associated with possible metal-ions release have led to the introduction of and shift towards all-ceramic restorations (3).

1.1.1 Metal-Ceramic Restorations

Metal-ceramic restorations is a relatively new term in prosthodontics that replaces the "old" porcelain fused to metal (PFM) term. The restorations are composed of a metal-coping that is overlaid with ceramic. Metal-ceramic restorations have a good long-term clinical performance record in dentistry (4). However, the failures rates of metal-ceramic restorations in fixed partial dentures (FDP) was reported to be 4 % after five years, 12 % after ten years and 32 % after fifteen years (5).

The main point for the compatibility between the ceramic and metal alloy is the construction of metal-ceramic restorations. The coefficients of thermal expansion (CTE) of the metal-coping should be slightly greater than that of ceramic veneer to induce low compressive stresses in the ceramic and prevent crack propagation during cooling and function (6). The acceptable range of difference in CTE between the metals/alloys and ceramic is considered to be $0.5 \times 10^{-6}\ ^{\circ}C^{-1}$ to $1.0 \times 10^{-6}\ ^{\circ}C^{-1}$ (7).

Metal-ceramic restorations cannot transmit light, which negatively affects the aesthetic outcomes of the restorations (6). Another disadvantage of metal-ceramic restorations is a possible allergic

reaction in some patients due to metal-ions release (such as Ni). To address aesthetic and biocompatibility issues, all-ceramic restorations were introduced (3).

1.1.2 All-Ceramic Restorations

Ceramics can be defined as "solid compounds composed in large part of inorganic non-metallic materials and are made by mixing the solid components with the application of heat to form solid crystalline structures" (8).

Ceramics are not considered new materials, as they were used thousands of years ago during the Stone Age (9). In 1723, Pierre Fauchard described the process of “enameling” metal denture bases (1). In 1789, the first porcelain denture tooth was introduced by De Chemant, a French dentist (9). In Paris, in 1808, Fonzi introduced "tetra-metallic incorruptible," which referred to porcelain teeth with embedded platinum pins (9). After that, the first ceramic crown was made and introduced by Dr. Charles Land in 1903 (10).

All-ceramic restorations are biocompatible and have good long-term stability intra-orally. In an all-ceramic restoration, the ceramic material could be monolithic or composed of a ceramic core that is covered with a glass-ceramic veneer, which is referred to as a bi-layered all-ceramic restoration (6), (9). In bi-layered all-ceramic restorations, the ceramic core supports the restoration and provides strength, while the veneer determines the final shade, shape, and aesthetics (6). The core also plays a significant role in developing the final restoration. The veneer-core bond strength is considered to be the weakest bond in bi-layered all-ceramic restorations (12) rendering the restorations more prone to delamination and fracture (13). The bi-layered all-ceramic restoration is usually used in aesthetic areas. The main disadvantage of such restorations is the delamination and fracture of the veneer. Moreover, a well-constructed occlusal contact with opposing teeth is

sometimes challenging to achieve. Finally, the compatibility of the core and veneer materials is critical to maximize the longevity of restorations (6).

Since monolithic restorations are composed of one ceramic material, they are more durable than the bi-layered ceramic restorations (12). Furthermore, proper occlusal morphology and contacts can be achieved using the pressable or computer-aided design and computer-aided manufacturing (CAD/CAM) method. However, the esthetic outcome from this type of restoration is inferior to that achieved by the bi-layered method (14). Therefore, monolithic ceramic restorations may be recommended when aesthetics are not a major concern and are, therefore, more suitable for restoring posterior teeth than anterior teeth (6).

1.1.2.1 Classification of Dental Ceramics

Several classification methods are used for dental ceramics, one of which is based on their composition. The composition-based classification is simple to understand and provides essential information that helps dental personnel to select suitable ceramics restorations (6). According to this criterion, dental ceramics can be divided into glass-based, glass-infiltrated, and non-glass-based (polycrystalline) ceramics (6).

1.1.2.1.1 Glass-Based Ceramics

This type of ceramics will be further divided into three sub-groups according to the percentage of added particles. These subgroups are: predominantly filled, moderately filled, and highly filled glass.

1.1.2.1.1.1 Predominantly Glass (Feldspathic Glass)

The feldspathic glass class consists mainly of glass with varying amounts of different kinds of particles. The percentage of added particles is less than 17 %. The flexural strength of this type is the weakest among ceramic materials, around 70 MPa to 90 MPa (15).

Feldspathic glass is one of the most aesthetically-pleasing ceramic types (6). It can be used to create veneers, inlays, onlays and veneers for cores and frameworks for all-ceramic restorations (bi-layered).

1.1.2.1.1.2 Moderately Filled Glass Ceramic

The second type of glass-based ceramics has a higher percentage of particles in comparison to the predominantly glass-ceramics. It contains up to 25 % of particles, such as leucite (16). The increasing percentage of the particles helps improve the mechanical properties of this class (6). However, it may lead to less aesthically pleasing results than the predominantly glass-ceramic types.

Moderately filled glass ceramic can be used as veneers, inlays, onlays, and veneers for metal copings and frameworks (13).

1.1.2.1.1.3 Highly Filled Glass Ceramic

These are glass-based ceramics in which the percentage of the particles ranges between 45 vol% to 70 vol%(6). Leucite and lithium disilicate are the most commonly used crystalline particles in this category. The flexural strength of leucite-based glass-ceramics ranges between 120 MPa to 160 MPa, whereas that of lithium disilicate-based glass-ceramics ranges between 300 MPa to 500 MPa (15). They can be used as inlays, onlays, veneers, and crowns (anterior and posterior) (17). Moreover, this type can be used as short-span, three-unit FDPs (18), or as core materials for crown and three-unit anterior FDPs (19).

1.1.2.1.2 Glass-Infiltrated Ceramics

This type of ceramic is considered glass-based ceramic but classified separately because it is based on ceramic cores, such as alumina or zirconia, which are infiltrated with glass (20). This type is known as In-Ceram (6). Based on the composition of the ceramic core, there are three different

sub-types: In-Ceram® Alumina, In-Ceram® Spinell (magnesium aluminate spinel), and In-Ceram® Zirconia (all from Vita) (6). In-Ceram® Alumina contains about 70 vol% alumina and 30 vol% glass matrix. The fracture toughness and strength are close to the those of pure polycrystalline alumina (13), (21). In-Ceram® Alumina does not have highly-aesthetic properties. (2). However, it demonstrates good flexural strength of about 600 MPa and can be used as a single crown and three-unit anterior fixed partial dentures (FPDs).

In-Ceram® Spinell is a modification of In-Ceram® Alumina. It contains magnesium spinel with trace amounts of alumina. It is more translucent but weaker compared to In-Ceram® Alumina and In-Ceram® Zirconia, with flexural strength around 350 MPa (22). It is only used for anterior crowns.

In-Ceram® Zirconia is a mixture of zirconia and alumina (~20 vol% to ~50 vol%, respectively) (13). It is opaque, which limits its application to areas where aesthetics are not critical, such as posterior restorations.

Overall, In-Ceram ceramics can be used for crowns and anterior three-unit FPDs (23).

1.1.2.1.3 Non-Glass-Based Ceramic (Polycrystalline Ceramic)

The ceramics in this class do not contain glass, but rather contain alumina or zirconia. Both materials have good mechanical properties and are tougher and stronger than glass-based restorations. For example, the flexural strength for alumina is around 650 MPa, and ranges from 800 MPa to 1500 MPa (6) for zirconia. However, this type of ceramics are less translucent and more opaque than glass-based ceramics (13).

The following section provides an in-depth review of zirconia as a dental material.

1.2 Zirconia as Dental Biomaterial

Zirconia has proven to be a highly promising restorative material due to its biological, mechanical, and optical properties, which lead to its application in different types of prosthetic treatments (24).

1.2.1 History of Zirconia materials

"Zirconium" is the term that came from an Arabic word "Zargon", which means "golden color." Zirconium dioxide (ZrO_2), or zirconia, was accidentally identified by the German chemist Martin Heinrich Klaproth in 1789, when he was working on some gem-heating procedures. (25). Afterwards, zirconia was used as a pigment for more than two centuries. In the late sixties, the application of zirconia as a biomaterial in the medical field took off, and the first use of zirconia as a ceramic biomaterial was to create a ball head in total hip replacements (THR) (25). In the early stages of development, many combinations of solid solutions, such as: (ZrO_2–MgO, ZrO_2–CaO, ZrO_2–Y_2O_3) were tested for biomedical application (25). The introduction of yttria-stabilized zirconia, often referred to as yttria-stabilized tetragonal zirconia polycrystals (Y-TZP), was a big step in the development of zirconia-based biomaterials (24). Y-TZP has good flexural strength (1000 MPa), fracture toughness (~10 $MPa \cdot m^{1/2}$) and dimensional stability. In-vitro studies of the mutagenic and carcinogenic properties of zirconia ceramic confirmed that it did not affect human cells (26). In the 1990s, zirconia was used as endodontic posts and implant abutments (27). Due to the outstanding mechanical properties, white color and superior biocompatibility, zirconia has been used as an alternative framework for partial and complete coverage of all-ceramic crowns and FPD (24).

1.2.2 Microstructural Properties

Depending on the temperature, zirconia has three crystalline structures: monoclinic (M), tetragonal (T), and cubic (C), as shown in Fig. 1 (28).

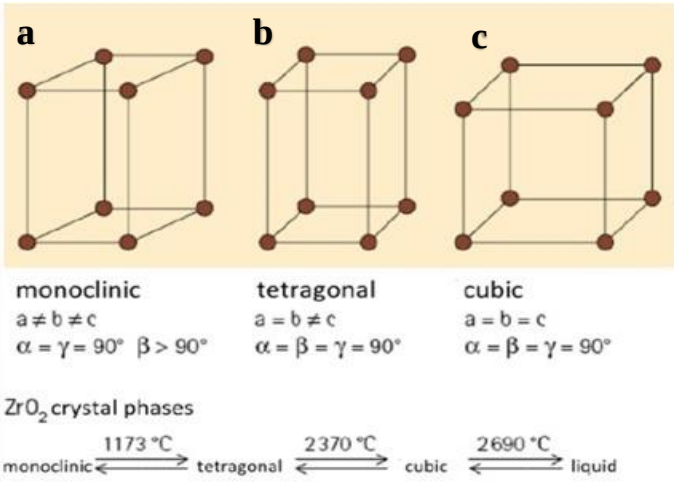

Figure 1: Crystalline phases and transition temperatures of zirconia: (a) monoclinic, (b) tetragonal and (c) cubic (28).

(Source: https://dx.doi.org/10.14288/1.0354411)

Zirconia, as found in nature, is in a monoclinic phase at room temperature and pressure. Zirconia transforms into the tetragonal phase when the temperature increases gradually up to 1170 °C, then into the cubic phase at 2370 °C (29). Whenever stress is applied to fracture zirconia, a stress-induced phase transformation occurs, from the metastable tetragonal to the monoclinic phase (accompanied with a 3.5 % to 5 % increase in volume), consequently increasing the resistance to crack propagation. (29). This is stress-induced toughening mechanism is illustrated in Fig. 2 (30) (31).

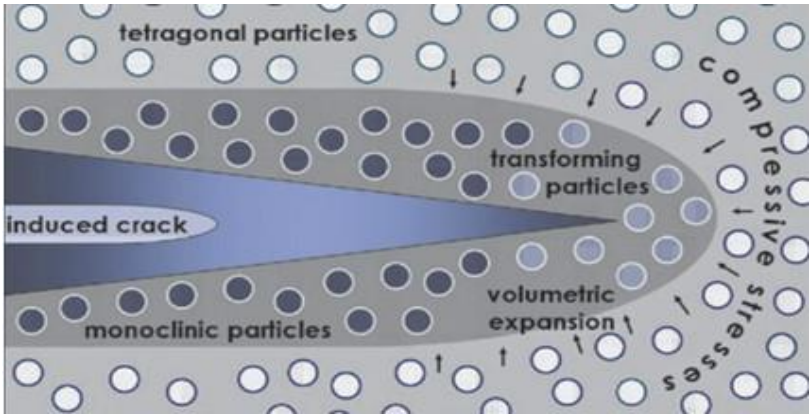

Figure 2: Schematic drawing of stress-induced toughening mechanism of zirconia at the crack tip (31).

1.2.3 Classification of Zirconia-Based Ceramics

Three types of zirconia have been widely used in dentistry, namely: magnesium partially stabilized zirconia (Mg-PSZ), zirconia-toughened alumina (ZTA), and the most commonly used is 3Y-zirconia (24) (32).

1.2.3.1 Zirconia-Toughened Alumina (ZTA)

ZTA is a material that combines alumina and zirconia , which can undergo stress-induced transformation to achieve excellent mechanical properties (33). The only ZTA product available in the market is In-Ceram Zirconia (6), which can be processed by slip casting or milling at the

pre-sintering stage (34). In-Ceram's porosity, however, is large, ranging between 8 % to 11 % (35).

1.2.3.2 Magnesium Partially Stabilized Zirconia (Mg-PSZ)

The microstructure of the Mg-PSZ contains clusters of tetragonal crystals impeded with cubic stabilized zirconia matrix (24). It has been reported that it is unsuitable for dental use because of its high porosity and large grain size (30 µm to 60 µm) (36). The Mg-PSZ has poor stability, which reduces the energy required for the T > M phase transformation (25) (37).

1.2.3.3 Zirconia 3Y-TZP

This is tetragonal zirconia polycrystal stabilized with 3 mol% of Yttria, or 3Y-TZP. This material is used for dental applications and has better mechanical properties than other ceramic biomaterials, such as alumina (28), as shown in Table. 1. It is also more aesthetically pleasing, as the color is matching that of natural teeth (29).

Table 1:Properties of some materials for biomedical applications (29).

Property	Units	Ti 6A1 4V	316 SS	Co Cr Alloy	TZP	Alumina
Young's modulus	GPa	110	200	230	210	380
Strength	MPa	800	650	700	900 - 1200	>500
Hardness	HV	100	190	300	1200	2200

3Y-TZP has better mechanical properties than other zirconia-based materials. It also has low porosity 1.5 vol% (38) and higher density 98.8% (39) (40). The grain size can influence the mechanical properties of 3Y-TZP. High temperatures and more extended sintering periods can

increase the grain size and negatively impact the mechanical properties (41). When the sintering temperature is high enough (1650 °C), grains are larger, in the 0.4 μm range (39). Grain size larger than 1 μm leads to a high T→M transformation rate, while lowering the grain size below 1 μm lowers the transformation rate (42). Additionally, zirconia with grain size below 0.2 μm does not undergo stress transformation toughening and hence its fracture toughness drops 8.4 $MPa.m^{1/2}$ (42). Consequently, the sintering process becomes a critical factor that needs to be emphasized and controlled throughout the production of dental restoration. (41).

1.2.4 Recent Advances in Zirconia Dental Materials

1.2.4.1 Monolithic Zirconia

When compared to the other ceramic and metal-ceramic restoration, monolithic 3Y-TZP restorations showed better long-term clinical performance (41), (42) and no deterioration of properties during long-term artificial ageing (44), (44). However, due to its opacity, monolithic zirconia restorations have inferior aesthetic properties compared to those of feldspathic glass-ceramics (41). To overcome this shortcoming, clinicians often use 3Y-TZP to fabricate crown cores and FDP frameworks, which are then veneered with translucent feldspathic glass-ceramics. However, chipping and fracture of the veneering ceramics, caused by processing-related residual stresses, was frequently observed in veneered zirconia restorations (45), (47). Chaar et al. (47) reported in their 10 y study that the observed cumulative chipping rate was around 37 %, while Rinke et al. (48) reported a lower 10 y success rate of around 57 %.

The opacity of Y-TZP has been modified by increasing the concertation of yttria (to 4 mol% and 5 mol%) and lowering that of alumina, along with increasing the sintering temperatures and reducing impurities (50). While this approach leads to an improvement in aesthetics due to an

increase in the cubic phase, it also leads to a decrease in mechanical properties, such as flexural strength (485 MPa) and fracture toughness (4.8 MPa.$m^{1/2}$) (51).

1.2.4.2 Multilayered Monolithic Zirconia

To further enhance the aesthetics of zirconia restorations, a multilayered zirconia system (MLZ) has been recently developed (51). The MLZ design aims to mimic the shade gradient observed in natural teeth, where the incisal area is translucent and an increase in chroma and opacity is achieved towards the cervical/gingival area (51). The first MLZ system was introduced in the dental market in February 2015 by Katana (Kuraray Noritaka, Japan). The system includes three different grades: Ultra Translucency Multi-layered Zirconia (UTML), Super Translucency Multi-Layered Zirconia (STML), and Multi-Layered Zirconia (ML). According to the manufacturer, these three material grades can cover all monolithic restorative applications encountered in a daily clinical practice. All three grades of this MLZ system are available as a discs ("puck") for in-lab milling, while the STML grade (4Y-TZP) is also available as a block for CEREC chairside milling (53). The flexural strength of the three grades, determined according to ISO-6872-2015 three-point bending test, is (460-557) MPa for UTML, (748-895) MPa for STML, and (1125-1194) MPa for ML (47- 48). The reported flexural strength of the STML block is (761-859) MPa (55). The three grades have different clinical applications: ML is recommended for long-span FPDs, UTML is recommended for veneers and single crowns, and STML for crowns and 3-units FPDs.

1.2.5. Methods of Fabrication of Zirconia

Over the last three decades (56), the CAD/CAM system has been expanding for routine use in the manufacturing processes. CAD/CAM fabricates restorations by subtractive manufacturing (SM), which is defined as "conventional machining in a form of subtractive manufacturing, in which a collection of material-working processes use power-driven machine tools, such as saws, lathes,

milling machines and drill presses, all of these are used with a sharp cutting tool to remove material to achieve the desired geometry physically" (56). In the early days, CAD/CAM had relatively poor quality and precision (55). The recent literature, however, shows promising results in the continuing enhancements of CAD/CAM, resulting in a gradual, full acceptance of the process for the fabrication of dental prostheses.

New developments and refinements in CAD/CAM along with developments in new materials have lead to a dramatic improvement in the quality and precision of obtained dental prostheses. Among those refinements is the perfecting of digital scanning systems and associated designing software.

Alongside developments in CAD/CAM systems, new materials emerged for dental prostheses fabrication. Since modern systems can handle a wide arrays of metals, ceramics and resins, high-strength materials, such as zirconia, can be used to produce metal-free restorations (57).

1.2.5.1 In-office Vs. Lab CAD/CAM

In comparing the in-office to the in-lab CAD/CAM process, the former, often referred to as the "full-chairside workflow", has become more competitive than the latter. In-office CAD/CAM restorations can be delivered in less than one hour. Furthermore, providing the restoration on the same day eliminates the need for provisionalization, which may lead to infection of the abutment teeth. Besides that, same-day procedures also eliminate the additional fees of the shipping to the laboratory and control the cross contamination associated with the milling process in the lab (58).

For the in-office digital workflow, the milling system consists of three major components, as shown in Fig. 3 (60):

1. Scanner: Scans the dental preparation produced by the dentist and can be intraoral or extra-oral. The surface data for the prepared tooth is scanned for a single crown. For FPD frameworks, additional occlusal characterization is required, such as data acquired from the adjacent teeth and the opposing dentitions, as well as centric occlusion.
2. Software/CAD: Used for the 3D planning and design of the restoration. The software helps design the virtual restoration on a virtual cast and then computes and digitizes the milling parameters.
3. Hardware/CAM: Computerized milling device used for converting the virtual restoration into the final dental restoration from a solid block of metal or ceramic. In most cases, some manual correction needs to be applied after the CAM fabrication. The dentist or dental technician must finish the restoration by polishing it and by applying, if necessary, staining colours or veneering materials.

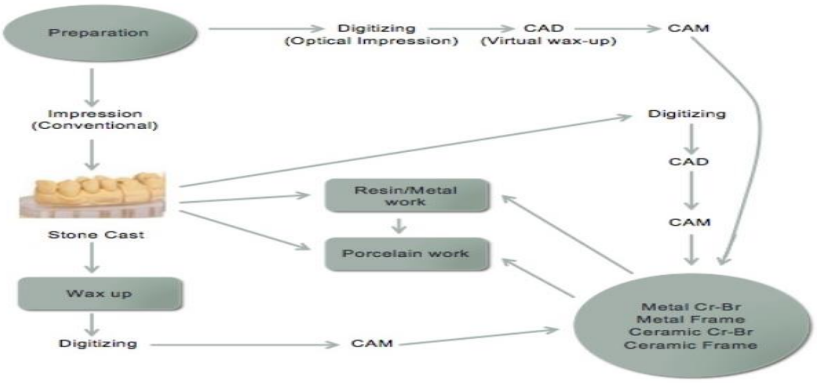

Figure 3: CAD/CAM workflow (61)

There are several in-office CAD/CAM systems available in the dental market, such as CEREC (Dentsply, Sirona), Planmeca E4D (Planmeca, USA, Inc.), Glidewell (Glidewell laboratories) and CS solutions (Carestream Dental). The most commonly used and tested in-office full-chairside CAD/CAM system is CEREC, as it had spearheaded the technology. The accuracy of

the in-office CEREC workflow has been tested, with literature reporting similar or better results than those of the traditional workflow (58).

1.3 Dental Bonding

Contemporary restorative techniques are based on bonding restorative materials or restorations to hard tooth structures (60). Adhesion is defined as intermolecular interactions that hold two surface together" (59). However, bonding to hard tooth structures involves not only adhesion, but also mechanical and chemical bonding. Following the pioneering approach of Buonocore in 1955 (61), researchers and manufacturers continue to improve the sealing and bonding capabilities of dental adhesives, which remains the most vulnerable link in restorative dentistry.

1.3.1 Dental Adhesive Systems

The three steps involved in any bonding procedure, i.e. preconditioning, priming and the placement of the adhesive, are present in dental adhesive systems as well. The role of preconditioning is to deliver a clean, uncontaminated surface and, if possible, to increase the surface area of the substratum. In dental bonding, the substrata can be hard tooth tissues, i.e. enamel and dentin, and restorative materials, i.e. metals, glass-ceramics, ceramics and resin composites. There are specific preconditioning agents and procedures for each one of these substrata. For enamel and dentin, the most commonly used preconditioning procedure is "total etching", which involves exposure to a silica- or polyvinyl alcohol-thickened 32 % to 37 % aqueous phosphoric acid gel for ~20 s, followed by rinsing and drying. Glass-ceramics are preconditioned by exposure to 4.5 % to 9 % hydrofluoric acid, followed by rinsing and drying, to provide an irregular, energy activated surface. The etching also provides many hydroxyl groups which can interact with primers for improved bonding with adhesives (62). Sandblasting with alumina particles is the recommended preconditioning procedure for metals, ceramics, and resin composites.

If necessary, primers are used prior to the application of the adhesive. The role of the primer is to change the surface chemistry of the preconditioned substratum, to render in chemically compatible with the adhesive. The primer facilitates wetting and may provide chemical bonding as well. There is no need to use primers for enamel or metals. The most commonly used primer for dentin is hydroxyethyl methacrylate (HEMA), an amphiphilic molecule that facilitates wetting of the hydrophilic dentin and can co-polymerize with the adhesive. Preconditioned glass-ceramics are primed with a silane coupling agent, which has three silanol groups that can bond to the feldspathic glass matrix and a methacrylate group that can copolymerize with the adhesive. For zirconia-based ceramic substrata, the most promising primer is 10-methacryloyloxydecyldihydrogen-phosphate (10-MDP), which has a terminal phosphate group able to interact with zirconia and a terminal methacrylate group that can copolymerize with the adhesive (66).

Dental bonding systems are classified (65) in four groups (Table. 2), based on the way the three steps involved in the bonding process are delivered: 1) Total-etch multi-step; 2) Total-etch two-step; 3) Self-etch two-step; and 4) Self-etch one-step. In the total-etch multi-step systems, the preconditioning, primer and adhesive are supplied in separate bottles and are applied in sequence. These systems have been shown to outperform all the others and are considered as the "gold standard" (63). In the total-etch two-step systems, the primer and adhesive are supplied in one bottle. It has been shown that "wet-bonding", i.e. leaving the dentin moist after preconditioning, is necessary in order to facilitate the penetration of the primer-adhesive combination into dentin. This requirement renders these systems technique-sensitive, since it is difficult to control the moisture level. In the self-etch two-step systems, acidic molecules/monomers are used to both precondition and prime the substratum. Their effect on enamel is inadequate and, since there is no rinsing involved, the possibility of continuous acid-etching of the substratum (67). In the self-etch

one-step systems, acidic molecules/monomers are combined with the adhesive and are applied simultaneously onto the substrata. These systems suffer from the same drawbacks as the self-etching two-step systems and have shown an inconsistent and tendentiously weaker adhesive performance, which depends on their specific formulation (68). To address the inadequate etching of enamel by the self-etching bonding systems, phosphoric acid etching of enamel has been recommended as an elective step.

The quality and stability of adhesive interfaces to enamel and to dentin play a significant role in the long-term clinical success of restorations.

Table 2: Classification of dental adhesive systems.

Category	Class	Etch	Priming	Adhesive
Etch-and-Rinse (ER)	Total etch 3-step	Phosphoric acid 32–40%	Primer	Adhesive resin
	Total etch 2-step	Phosphoric acid 32–40%	Primer + Adhesive resin	
Self-etch (SE)	Self-etch 2-step	Acidic monomers + primer	Adhesive resin	
	Self-etch 1-step	Acidic monomers + primer + adhesive resin		

1.3.2 Adhesion to Zirconia

Unfortunately, unlike glass-ceramics, zirconia is not suitable for etching with HF at temperatures, times, and concentrations available to dental practitioners. Flamant et al. etched the 3Y-TZP with 40 %HF for times up to two hours and examined the surface integrity, flexural strength and resistance to hydrothermal degradation (69). This approach, however, cannot be implemented in a dental office setting.

Mechanical methods, such as surface grinding or abrading, may be used to roughen the surface (70). However, these can create surface flaws that would reduce the strength of the zirconia (70).

Over the last few years, many adhesive protocols and techniques have been studied. Different treatments of zirconia surfaces, application of primers or adhesives, and various types of resin cements have been investigated. However, a standardized adhesive cementation protocol that provides reliable results has not been identified. Kern and his colleagues (71–73) confirmed that many bonding protocols for high-strength ceramics work in the short term. They have shown that strong and durable long-term resin bonds were achieved only after surface pre-treatment with air-particle abrasion and the use of an adhesive resin composite luting agent that incorporates phosphate monomers. It has been shown that 10-MDP can better wet air-particle abraded preconditioned zirconia surfaces and provide superior long-term bond strength (74). Therefore, a three-step approach, abbreviated it as the "APC zirconia-bonding concept", has been recommended to achieve a long-term durable bond strength to zirconia (74):

1. Step A: air-particle abrade the bonding surface with alumina or silica-coated alumina particles. This sandblasting preconditioning procedure could be achieved chairside by using a microetcher with small particles (50 μm to 60 μm) at a low pressure (below 0.2 MPa). The overall effect of alumina pre-treatment seems more important than actual surface roughening, especially with its ability to effectively decontaminate the bonding surfaces.
2. Step P: apply a zirconia primer, which is typically a phosphate methacrylate monomer, such as 10-MDP. 10-MDP has been shown to be effective to bond to metal oxides.
3. Step C: use a dual-cure or self-cure resin composite luting agent to ensure adequate polymerization/conversion beneath zirconia restoration.

1.3.2.1. Air Particle Abraded

Russo et al. published a systematic review of preconditioning methods of zirconia, focused on laboratory studies (75). The most commonly used protocol was sandblasting.

Sandblasting is a process that relies on the energy released by alumina (Al_2O_3) particles emitted at high-speed through a nozzle, the carrier being pressurized air. The impact results in the erosion of the substratum with the formation of a rough, clean, and wettable surface (76). However, sandblasting can lead to surface damage, defects and cracks. Therefore, the mechanical integrity of the zirconia could be affected and compromised. It is advisable to carry out sandblasting according to the recommended parameters of pressure, distance from the source, and particle size. In his study, Souza et al. (70) recommended carrying out the sandblasting process using smaller particles, around 30 μm, with moderate pressure of 0.25 MPa, to minimize material damages. On the other hand, Ozan et al. (77) proposed a protocol for blasting zirconia with alumina particles diameter between 30 μm to 50 μm, at a pressure between 0.05 MPa to 0.25 MPa for at least 20 seconds. The blast jet should be positioned 10 mm from the target and kept in motion to prevent creating any cracks or defects on the zirconia surface.

1.3.2.2 10-MDP as Zirconia Primer

In the mid-1970s, the Kuraray company introduced 10-MDP as a primer. Currently, 10-MDP is found to be one of the most successful primers for zirconia. The structure of 10-MDP is given in Fig. 4 (78):

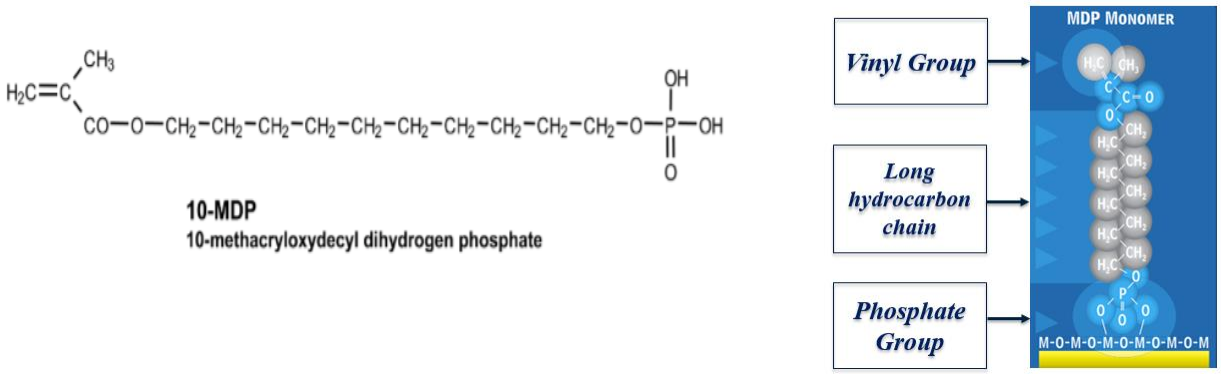

Figure 4: Structure of 10-MDP and its functional groups.

The terminal phosphate group reacts with zirconia and forms P-O-Zr bonds, while the methacrylate group at the other end copolymerizes with the RCLA. These two functional groups are separated by a 10 carbon chain, responsible for physical/chemical characteristics, such as viscosity, rigidity, hydrophobicity, and solubility (75).

Chemical bonding between 10-MDP and Y-TZP has been extensively studied. Kern and Wegner (71) were the first to report the long-term bond strength of phosphate monomer containing resin-based composite cement to ZrO_2. They compared the tensile bond strength of particle air-abraded ZrO_2 to several bonding systems. After 150 days, it was determined that only the two 10-MDP-containing cements exhibited high bond strength [Panavia: (49.7 ± 8.1) MPa; Panavia 21: (46.0 ± 7.4) MPa] and showed no significant difference in bond strength after artificial ageing. Further work conducted by Wegner and Kern (73) on the 2 y tensile bond strength of resin cements to

ZrO_2 confirmed that the functional phosphate ester group of 10-MDP forms a water-resistant chemical bond with zirconia. Therefore, 10-MDP-containing resin cements are recommended for bonding of ZrO_2 in clinical settings.

However, the pure 10-MDP is a sticky colloid and its molecular structure is too crowded for it to be optimally dispersed in the non-solvated form on the surface of Y-TZP. Accordingly, a solvent, such as ethanol or acetone, is required to facilitate the optimal dispersion of 10-MDP. As Chen et al. mentioned in their study, the optimal concentration range of 10-MDP ranges between 5 % to10 % (79). Also, de Souza et al. (80), concluded that an experimental 10-MDP-containing primer solution (0.5 % 10-MDP in ethanol),lot number 110114/expiration date 11-2012; Kuraray), has a great affinity to zirconia. In another study done by Yoshida et al. 2006, 10-MDP monomer was used at (0.1, 0.2, 0.5, 1.0, and 5.0) wt.% in ethanol. Regardless of the concentration of 10-MDP, the bond strength was more robust than that of groups not treated with 10-MDP primer (81). Camphorquinone (CQ), a free-radical polymerization photo-initiator, along with 4-dimethylaminobenzate (EDMAB) as co-initiator, in a 1:2 to 1:3 molar ratio of CQ to amine, are

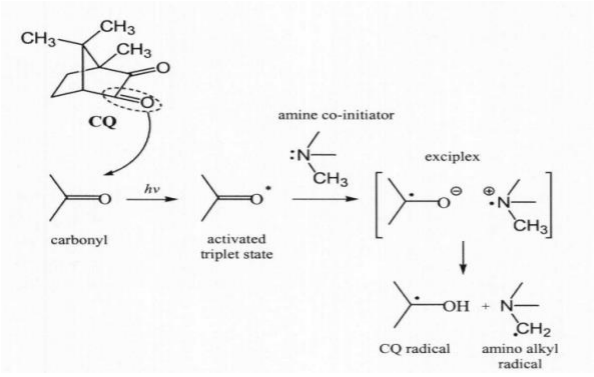

Figure 5: Structure of CQ and visible light-activated free radical generation pathways (83

added to 10-MDP to maximize the degree of conversion (80). Figure 5 illustrates the structure of CQ and visible light activated free radical reaction pathways (80) (82).

1.3.2.3 Resin Composite Luting Agents (RCLA)

Dual or self-cure RCLA should be used to ensure adequate polymerization/conversion beneath zirconia restorations (74). A review done by Blatz et al. (75) concluded that RCLA are the material of choice for the adhesive luting of ceramic restorations. In general, the RCLA have compositions similar to conventional restorative resin composites and consist of inorganic fillers embedded in an organic matrix, such as Bis-GMA/TEGDMA/UDMA. RCLA can be classified according to their activation mode, as auto polymerizing (chemically activated), photo-activated, or dual activated materials (83). Photo-activated RCLA offer a wide variety of shades, consistencies and compositions. Clinical application is simplified through long handling times before and rapid hardening after exposure to the light. Shade, thickness, and transmission coefficient of ceramic restorations and RCLA influence the conversion rate of the photo-activated material. Dual-activated RCLA offer extended working times and controlled polymerization (83), while chemical activators ensure a high degree of polymerization. Most dual-activated RCLA still require photo-polymerization and demonstrated lower hardness when it was omitted (84,85).

1.4 Testing of Adhesion

Adhesive interfaces have been tested using different methodologies to predict their clinical performance. This section will provide an overview and critique of the most common bond strength tests used in dental research.

1.4.1 Bond Strength Testing

Bond strength can be considered a measure of the adhesive forces between two interfaces and has traditionally been considered an essential characteristic and predictor of the success of dental restorative materials. Traditionally, several mechanical tests have been used to assess it.

Bond strength testing could be accomplished by loading of a test specimen in either shear (shear bond strength – SBS) or tension (tensile bond strength test – TBS), until failure. Based on the dimension of the tested bonding area, the tensile and shear bond strength tests are classified as macro (mm^2 range) or micro (μm^2 range). The International Organization for Standardization (ISO) technical specification ISO/TS 11405 summarizes the recommendations for sample preparation and testing. However, the details regarding the bonding area, testing assemblies and loading conditions are vague. Consequently, the different bond strength experimental research protocols vary significantly among studies. Therefore, comparing results from various studies is quite difficult (86).

SBS technique has the advantage of being an easy and quick testing method that requires no additional specimen processing for the post-bonding procedure. It is easy to perform, involving minimum equipment and simple specimen preparation. TBS is less common due to the more time-consuming methodology and laboratory sample preparation (87).

SBS has several limitations and flaws. Many variables that influence the specimen design and test mechanics have been identified (86). For example, the bonding area is variable among studies and directly affects the bond strength. The greater the bonding area, the lower the bond strength because of the higher probability of finding critical size defects. Additionally, the loading type and test design were found to significantly impact SBS values (86). An important limitation SBS is that the shear stress distribution was found to be lacking uniformity and was not concentrated at the interface, which questions the validity of the test (88).

Even when keeping the geometric design and adhesive interface identical, the results of SBS testing differed upon the modification of the specimen outline (89). In other words, modifying one of the parameters inherent to the SBS testing method resulted in an evident effect on the outcome.

To further demonstrate the wide variety of experimental protocols among the studies, in a recent survey of 100 SBS and TBS studies published from 2007 to 2009, the authors found no consensus of the parameters discussed previously (86).

In 1994, Sano et al. developed the μ-TBS (90). It differs from the macro-TBS in the size of the bonding area, being much smaller, at ~1 mm^2 or less. As in the case of SBS tests, any change in the testing parameters, such as the specimen shape, bond area, and gripping device specification might result in different outcomes, rendering the comparisons of results from different difficult. For instance, in a survey conducted by Armstrong et al. of 90 published papers of μ-TBS studies, they found that only 10 % described the experimental protocol in detail (91).

The μ-TBS testing has several advantages over other bond strength tests. It has a more uniform stress distribution at the adhesive interface and minimizes interfacial defects (90). It has fewer cohesive failures, and the bond strengths are higher than those measured from macro-bond strength testing, due to the lower probability of defects to be present at the bond interface. Moreover, accelerated environmental ageing by storage in water is available due to the short diffusional distance (91).

Some limitations include more laborious specimen preparation, with a considerable amount of pre-testing failure (87). In addition, specimens are harder to fabricate with consistent geometry and surface finish without special equipment. In addition, specimens could be easily damaged and dehydrated (92).

In conclusion, bond strength tests have severe limitations and do not permit the assessment of the adherence provided by different bonding systems. In summary, as stated by Alamar and Blatz, the validity of a BST is highly questionable because “no amount of standardization will overcome inconsistency problems if a test is fundamentally flawed” (93).

1.4.2 Fracture Mechanics

Fractures mechanics is its alternative approach for bond strength tests (91). It has been proposed to measure the intrinsic adhesive interfacial properties (91). Specifically, the fracture mechanics approach concentrates on studying the failure of a bond interface by crack initiation and propagation and could be a more predictable and appropriate test for assessing adhesion (94).According to Anusavice et al., adhesion can be defined as “the attractive intermolecular interactions creating a bond between the boundaries of two materials,” while cohesion can be defined as “the attractive forces between the molecular constituents within a material” (9). Mode of the failures was classified according to the Scherrer et al. (90). Failure of an adhesive interface can occur in several modes, as illustrated in Fig. 6. In valid tests, only adhesive (Fig. 6 a and b), cohesive (Fig 6 c) and mixed (Fig. 6 d) failure modes should occur.

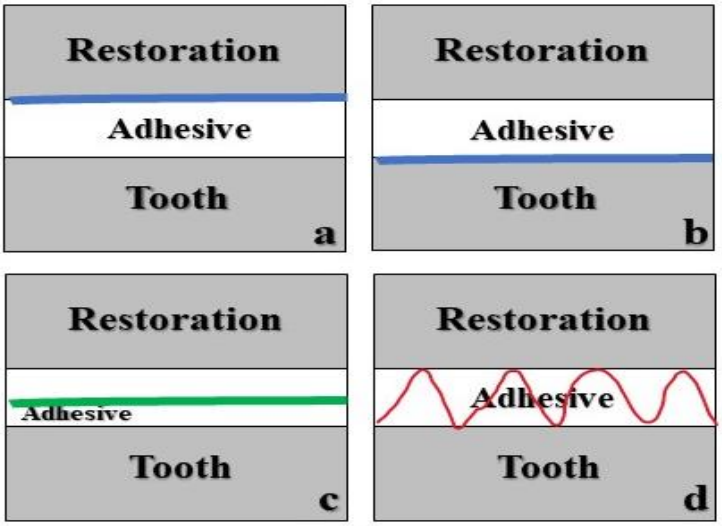

Figure 6: Possible failure modes: (a) adhesive (interface restoration-adhesive), (b) adhesive (interface tooth-adhesive), (c) cohesive in adhesive and (d) mixed (restoration-adhesive-tooth) (90)

During the loading of an adhesive joint, the adhesive and bonding substrate are deformed by the applied forces, disrupting the adhesive bonds at the interface, and creating new surfaces. Fractures or failures could occur when the applied forces generate enough energy to surpass the work of adhesion by breaking the interfacial bonding. This is dependent on the number and type of bonds disrupted at the interface. The fracture mechanics approach measures the energy needed to create fracture surfaces in a controlled environment. This concludes that the fracture mechanics measures the intrinsic adhesive properties, independent of joint geometry (95).

Fracture toughness is defined as "the resistance of a brittle material to crack propagation from existing defects/flaws under an applied force" (96). In 1964, Irwin et al. identified the parameter representing the stress around a sharp crack in a linear-elastic material (95), called the stress intensity factor *K*, a factor that is independent of the material. Fracture occurs when the value of the K exceeds a critical value, denoted K_c (95). The latter is an inherent material property (95).

Also, Irwin et al. (95) classified the different loading modes that can be applied to test specimens:

1. Mode-I - tensile forces.
2. Mode-II - shear forces.
3. Mode-III - torsional forces.

Therefore, K_{IC} represents the critical stress intensity factor value in tension for crack growth. This value is referred to as fracture toughness. Multiple test conformations are available to evaluate K_{IC}. One of these approaches is the chevron-notched short rod (CNSR) test, introduced by Baker (96). The test involves cutting a chevron notch inside a cylindrical specimen. However, specimen preparation could be technically challenging and time-consuming, especially for dental materials.

In 1996, Ruse et al. (97) introduced an innovative approach for evaluating K_{1C} and interfacial fracture toughness (IK_{1C}) using a notchless triangular prism (NTP) specimen that, when placed in the specimen holder, replicates the configuration of the standardized CNSR test. This method overcomes the difficulties of the CNSR specimen preparation and has been recognized as a valid alternative (95) (97).

The method involves an NTP specimen of dimensions (6x6x6x12) mm or (4x4x4x8) mm secured in a custom specimen holder A defect of approximately 100 μm is introduced at the level of the adhesive interface, under magnification, to enable crack initiation. The assembly is then loaded in tension at a cross-speed of 0.1 mm/min until fracture or crack arrest (97).

The value for K_{IC} is calculated using the standard formula:

$$K_{IC} = \frac{P_{max}}{DW^{½}}\ Y^{*}_{min} \qquad (1)$$

Where:

P_{max} is the maximum load recorded during testing, D is specimen diameter, W is specimen length and Y^*_{min} is the dimensionless stress intensity factor, equal to 28 (97).

1.5 Clinical significance

The bond to hard tooth tissues plays a large role in the long-term clinical survival of zirconia restorations. This study aimed to address the scarcity of data regarding the suitability of 10-MDP to mediate adherence of RCLA to recently introduced high translucency monolithic zirconia materials.

Chapter 2: Research Question and Specific Aim

2.1 Definitive Aims

This study aimed to apply fracture mechanics methodology to investigate the effect of 10-methacrylooyloxydecyl dihydrogen phosphate (10-MDP) on the adherence of a resin composite luting agent (RCLA) to rapid-fired zirconia (RFZ).

2.2 Research Question

Does 10- MDP affect the adherence of a RCLA to RFZ?

2.3 Research Hypothesis

Null Hypothesis (H_0): 10-MDP does not influence the adherence of a RCLA to RFZ.

Chapter 3: Materials and Methods

3.1 Materials:

The materials used in this study are presented in Table 3.

Table 3: Experimental Materials.

Rapid Fired Zirconia	**KATANA™ ZIRCONIA BLOCK-STML-fast sintering (KURARAY)** **Ref: 125-6602**
5 % 10-MDP ethanol primer **(Made in house)**	**5% Ethanol LOT: 10754-820** **10-MDP (10-phosphonooxydecyl methacrylate) LOT: LC49861** **CQ (Camphorquinone) LOT: AG40872** **EDMAB (Ethyl 4-dimethylamino benzoate) LOT: 10D9M88J**
Silane Coupling Agent	**Bisco® Bis-Silane (2-part porcelain primer)** **Bottle A: (5-10%) 3-(Trimethoxysilyl)propyl-2-Methyl-2-Propenoic Acid and (85%) Ethanol** **Bottle B: (1-5%) Phosphoric Acid, conc=85% and (30-50%) Ethanol** **LOT: 2000003666 (USA)**
Resin Composite Luting Agent	**RelyX™ Veneer** **(3M ESPE)** **LOT: 7614A3**

3.1.1 KATANA™ ZIRCONIA BLOCK-STML

The KATANA zirconia blocks are pre-sintered zirconia blocks designed for CEREC milling systems, in-house or laboratory (external use). The blocks are available in three different sizes: 12Z, 14Z and 14ZL. Super Translucent Multi-layered (SRML) 14ZL blocks were used in this study.

Figure 7: Possible failure modes: (a) adhesive (interface restoration-adhesive), (b) adhesive (interface tooth-adhesive), (c) cohesive in adhesive and (d) mixed (restoration-adhesive-tooth) (90)

The material is composed of zirconium dioxide (ZrO_2) with yttrium oxide (Y_2O_3). They are classified as type II/ class 4 dental ceramics (ISO: 6872:2015). The coefficient of thermal expansion (CTE) of the material, between 25 ^oC and 500 ^oC, is $9.8x10^{-6}$ /K. Fig. 7 shows a KATANA zirconia block used in this study.

3.1.2 10-MDP

Many commercial adhesives, primers and adhesive RCLA contain 10-MDP, along with other ingredients. The application of primers containing 10-MDP significantly enhances bonding and durability. In this study, a light-curable 5 % 10-MDP in ethanol was prepared freshly in house. The required quantities were calculated by weight percentage (wt. %) (Table 4), were measured with an analytical balance, were dissolved in chromatographic grade ethanol in a 10 mL analytical

flask, and the volume was brought to mark. The ingredients and the freshly mixed 10-MDP are shown in Fig. 8.

Figure 8: 10-MDP AK Scientific Inc.

Table 4: 10-MDP Primer composition.

Ingredients	wt. %	Actual quantities
10- Methacryloyloxdecyl-dihydrogen phosphate (10-MDP)	9.660	0.966 g/10 mL
Camphorquinone (CQ)	0.166	0.0166 g/10 mL
Ethyl 4-(dimethylamino)benzoate (EDMAB)	0.579	0.0579 g/10 mL

3.1.3 Bisco® Bis-Silane

Bis-Silane is a two-component system silane coupling agent used to enhance bonding of resin composites to feldspathic materials. For the case of one component systems, clinical research indicated that they tend to be polymerized near the end of their shelf life. The two components

silane system offers a more stable approach to ensure adequate bonding. Bis-Silane is an ethanol-based product that is less harmful than other acetone-based silane agents.

Silane is a dual function monomer, consisting of three silanol groups aimed to react with the surface of feldspathic materials and a methacrylate group aimed to co-polymerize with the resin matrix of the composite. In general, silane coupling agents are well known for enhancing the wettability of feldspathic substrates by resin composites, increasing physical, mechanical, and chemical bonding and imparting greater resistance to water attack at the boding interface.

Two components system of Bis-Silane (Fig. 9) from Bisco® contains a non-hydrolyzed silane (first bottle) and acidic water (second bottle), which are supplied separately and mixed in equal volume before their application. When the two components are mixed, freshly hydrolyzed silane is formed, with the mixed solution remaining mildly acidic.

Figure 9: Bisco® Bis-Silane (Two Component)

3.1.4 RelyX Veneer (3M. ESPE)

RelyX Veneer (3M. ESPE; Fig. 10) is a light-curable methacrylate RCLA, delivered as a single component. It contains a resin system consisting of triethylene glycol dimethacrylate (TEGDMA) and bisphenol-A- diglycidylether dimethacrylate (Bis-GMA) monomers. The methacrylate monomers are blended with zirconia/silica filler, with a particle size range of (0.2-3) μm and a volume percentage of approximately 47 %. RelyX Veneer, not having any functional groups to enable it to chemically bond to substrata, is designed to be used with adhesive systems.

RelyX Veneer is thixotropic, allowing it to flow easily under pressure, hold the shape, and stay in place until light-curing occurs. In addition, it contains pigments and a highly efficient photo-initiator system activated by visible blue light, in the (400 to 500) nm range, with a minimum irradiance of 400 mW/cm^2.

RelyX Veneer was selected because it cannot bond by itself to zirconia and it can be light cured between the NTP half-length specimens, where the maximum distance is just slightly over 2 mm.

Figure 10: RelyX™ Veneer (3M. ESPE)

3.2 Methods

3.2.1 Sample Size Calculation

Lehr's sample size equation was used in a power analysis calculation to determine sample size (*n*) needed for the K_{IC} test with $\alpha = 0.05$, power of 80 % and standardized difference (Δ) of 1.08. Lehr's basic formula was used to obtain *n* value:

$$n = \frac{16}{\Delta^2} \quad (2)$$

Where

$$\Delta = \frac{\delta}{\sigma} \quad (3)$$

In the above equation, Δ is the standardized difference, δ is the treatment difference (between two means), and σ is the standard deviation. To detect a difference of 25 % between means was considered clinically significant. The calculated sample size was 13.

The experimental design is summarized in Table. 5

Table 5: Experimental Design

Groups (78 samples)	**Materials used**	**Testing**	
		24 hours	90 days
Group 1 (Control)	Both halves RC	n =13	n =13
Group 2	Both halves 10-MDP	n =13	n =13
Group 3 (Negative control)	Both halves Silane	n =13	n =13

The flow chart (Fig. 11) shows the experimental design.

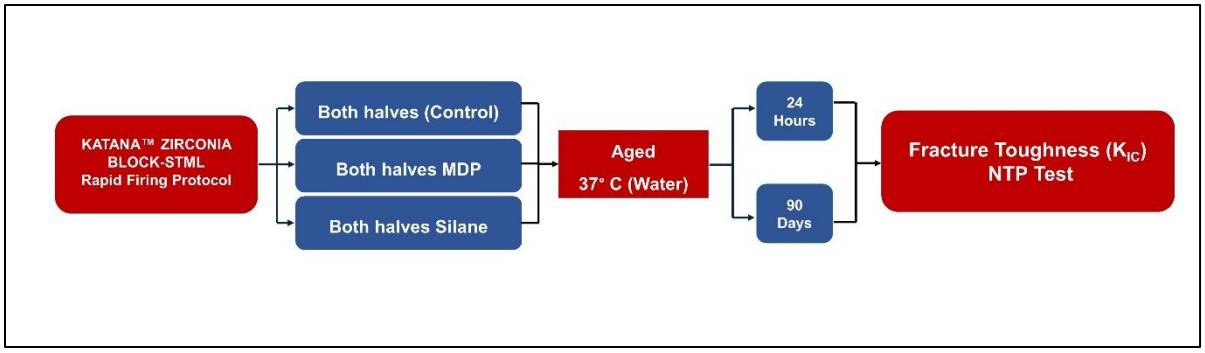

Figure 11: Experimental design.

3.2.2 Sample Preparation

3.2.2.1 KATANA™ ZIRCONIA BLOCK-STML

KATANA blocks, delivered as pre-sintered blocks, were first removed from their packaging box and inspected for any irregularities. In the next step, the metal stem required by the milling system was cut using slow-speed Isomet saw (Buehler, Lake Bluff, USA), under constant water irrigation, equipped with a 0.014 MK-303 Professional lapidary blade (MK Diamond Products, Inc., Torrance, U.S.A.) Fig. 12.

Figure 12: Removing milling system metal stem from the KATANA block.

Then, the blocks were secured longitudinally, with two-sided tape, onto the specimen holder and precisely cut into two halves (Fig. 13).

Figure 13: KATANA block cutting in two halves.

Each half was then secured with two-sided tape to a custom-fabricated jig (UBC Faculty of Dentistry, Vancouver, Canada), allowing 60° angles cuts in different orientations (Fig. 14).

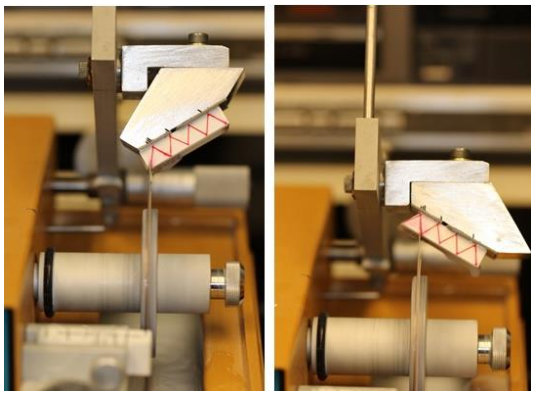

Figure 14: Katana half-block cut at 60° angle using a custom jig

All sections were made with a low-speed Isomet saw under constant water irrigation and with a 0.014 MK-303 Professional lapidary blade (Fig. 15). The blade was cleaned regularly and changed whenever the cutting efficiency was deemed inappropriate.

Figure 15: Isomet saw and Lapidary blade.

The obtained prisms were further wet ground and polished using a custom grinding/polishing jig (UBC Faculty of Dentistry, Vancouver, Canada) and 320 and 600-grit SiC abrasive disks under constant water irrigation on a Metaserv wheel grinder (Buehler, Lake Bluff, USA) (Fig. 16).

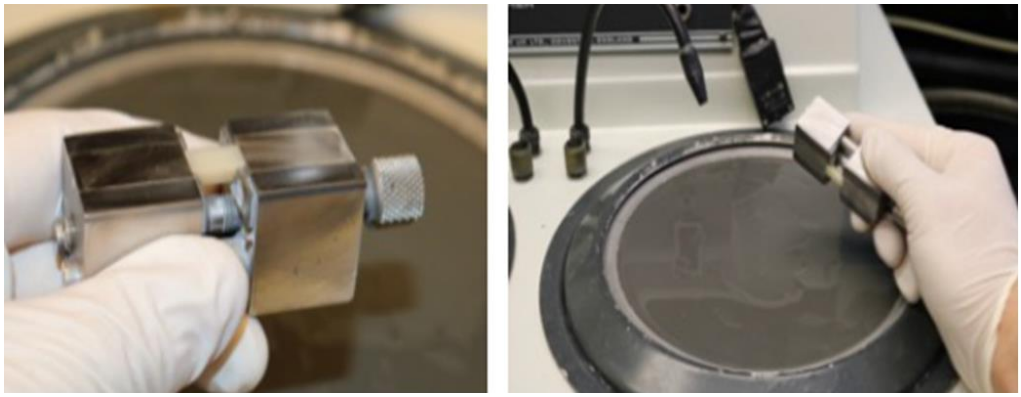

Figure 16: Prism specimen grinding and polishing.

The final dimensions of the prisms (Fig. 17) after polishing were (7.5 x 7.5 x 7.5 x 15) mm, with height of 6.5 mm, to accommodate ~25 % shrinkage of the blocks during sintering, as indicated by the manufacturer.

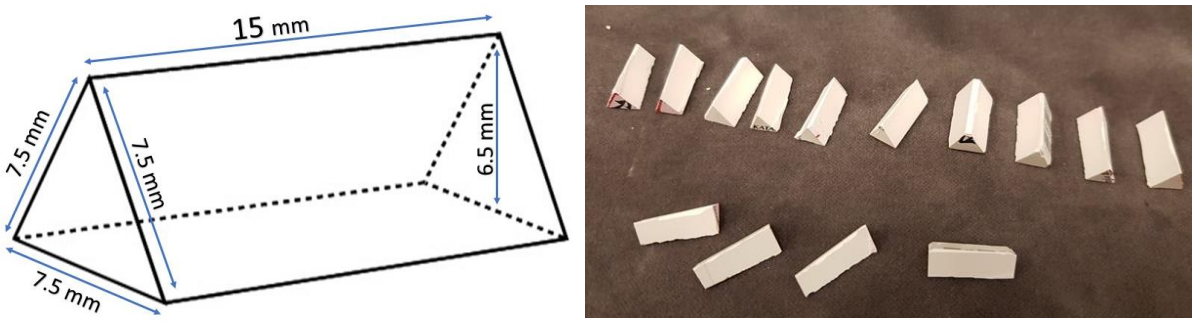

Figure 17: Prism specimen dimensions and prepared NTP specimens, pre-sintered.

3.2.2.2 Fast Sintering Processing

All prisms' specimens were fast sintered using the Zircom sintering furnace (Rotsaert Dental laboratory, Hamilton, Ontario, Canada), following the manufacturer's recommendation (Fig. 18).

Figure 18: Zircom furnace to sinter the prism specimens.

Courtesy of Rotsaert Dental Lab, ON, CA)

As per manufacturer's recommendation, the prims were sintered in the dental lab setting using a Zircon furnace and the sintering program No. 3. The Zircom furnace could not match the recommended temperature change rate of 130 °*C* per min. A rate of 70 °*C* per min was used, reaching 900 °*C* in 13 min. The rest of the program matched the manufacturer's recommendations, as illustrated in Fig. 19.

Sintering program 3

Temperature	Programming Rate	Holding Time
Room Temp. — 900°C (1652°F)	130°C/min. (234°F/min.)	—
900°C (1652°F) — 1500°C (2732°F)	50°C/min. (90°F/min.)	—
1500°C (2732°F) —1560°C (2840°F)	15°C/min. (27°F/min.)	—
1560°C (2840°F)	—	16 min
1560°C (2840°F) — Room Temp. (*)	-70°C/min. (-126°F/min.)	—

*The restorations may be removed at 800°C (1472°F) or less depending on the circumstances.

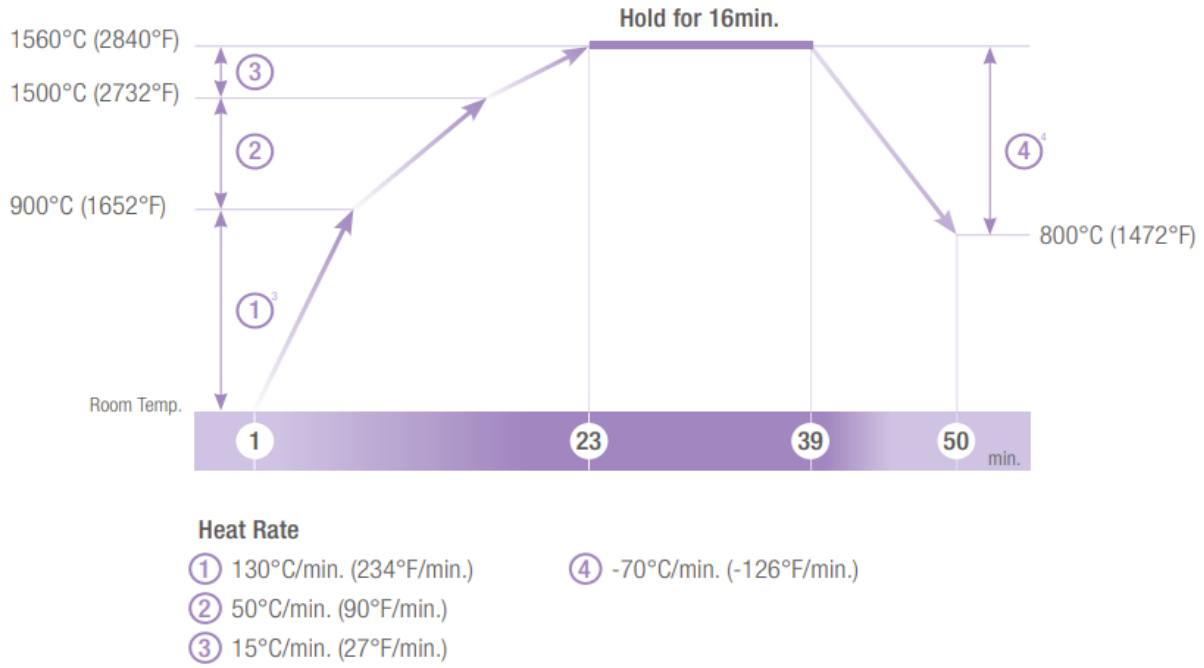

Figure 19: Sintering protocol as per manufacturer's recommendations.

In each cycle, only four specimens, placed horizontally to allow stable sintering during the shrinkage phase and not to impede airflow, were fired (Fig. 20).

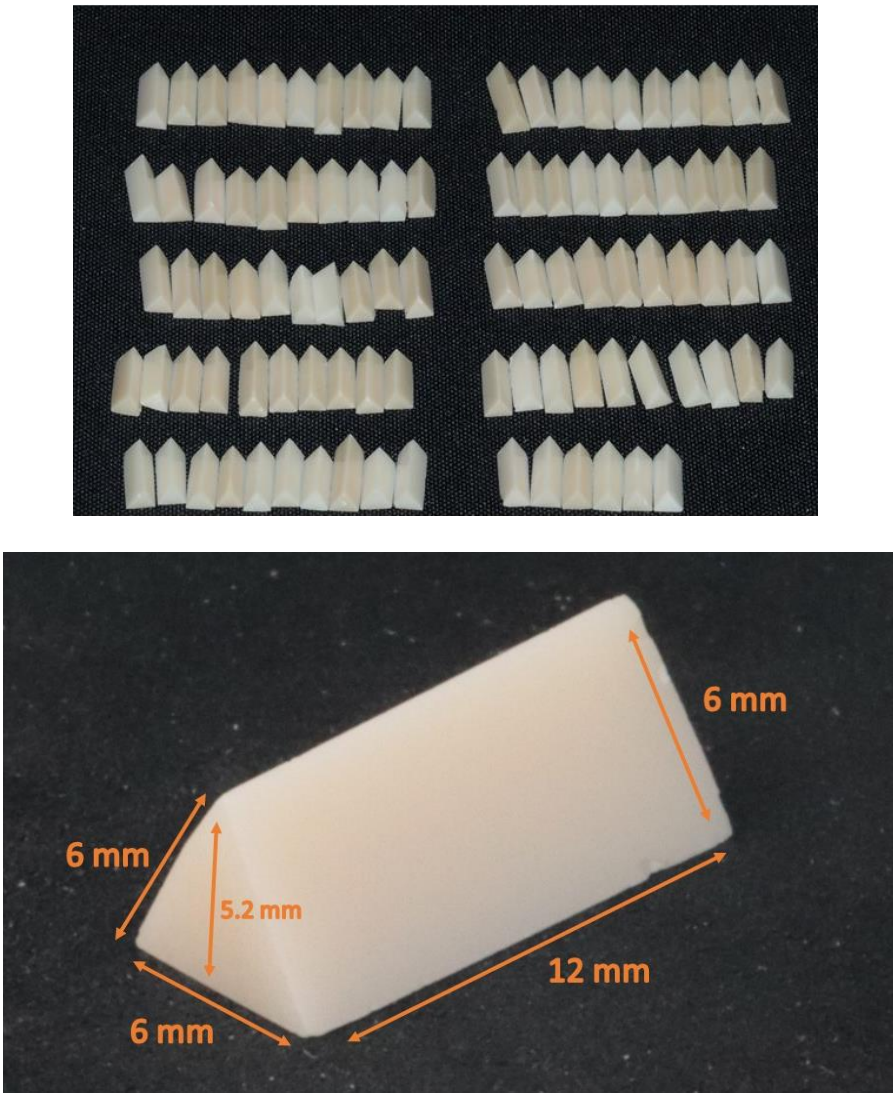

Figure 20: Sintered NTP specimen dimensions and fired specimens.

After sintering, each triangular prism was marked in the middle and end, as shown in Fig. 21A. Each prism was cut into halves, using a diamond blade mounted in a low-speed Isomet saw, under constant water irrigation Fig. 21B. Corresponding halves were marked to facilitate their alignment during the bonding process Fig. 21C

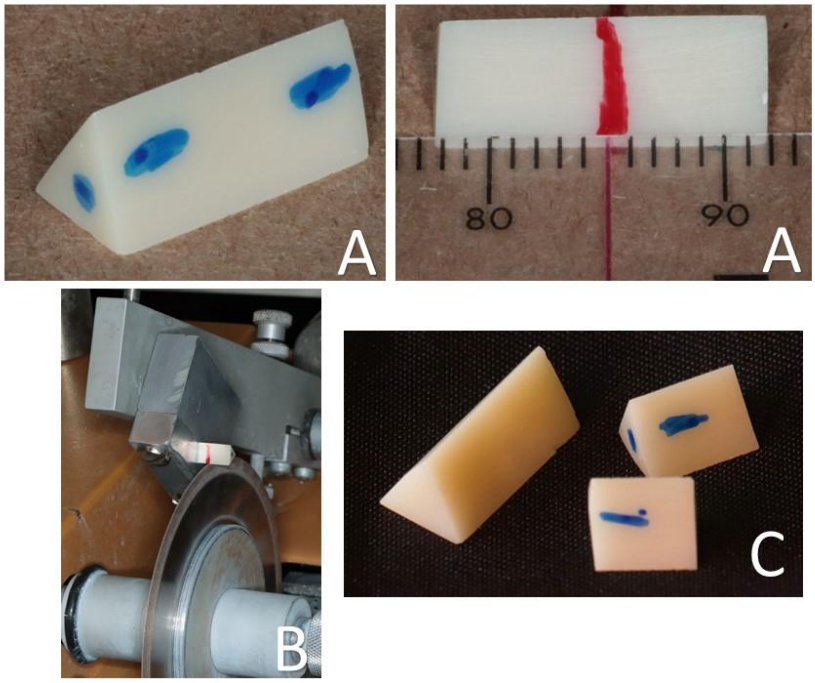

Figure 21: Prism specimen preparation for the cementation protocols. A: marked prism in middle and end of each specimen; B: cutting the prisms in two halves; C: Final two halves of the prism specimen.

3.2.2.3 Resin Composite Luting Agent

Four samples of (4x4x4x8) mm triangular prism specimens were prepared using a Teflon mould (UBC, Faculty of Dentistry, Vancouver, BC, Canada). The process was completed by first utilizing a mylar film to block one end of the jig, injecting the RCLA into the mould, and placing a second mylar film on the other end (Fig. 22A). Each end was then light-cured (3M Elipar S10 LED Curing light 76952 3MESP, wavelength = 430-480 nm, intensity = 1470 mW/cm^2) for 60 s before removing the sample from the mould (Fig. 22B). Finally, each surface of the triangular prism was light-cured for an additional 60 s (Fig. 22C) and allowed a total setting time of 6 minutes before storage in water at 37 *ºC* (Fig. 22D).

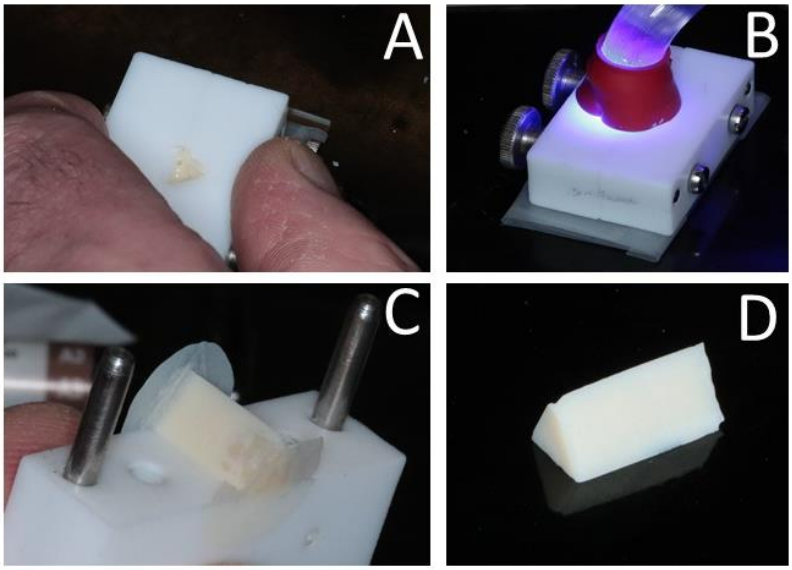

Figure 22: A: RCLA being dispensed into the plastic mold; B: Light cure each end; C: removed the plastic mold and light cure each side; and D: RCLA prism specimen.

3.2.3 Cementation Protocols

The adhesive surface of all half-prisms was ground using 600 grit SiC abrasive disks. Each of the two halves of one prism were marked on one of their surfaces to ensure proper alignment during the cementations process (Fig. 23).

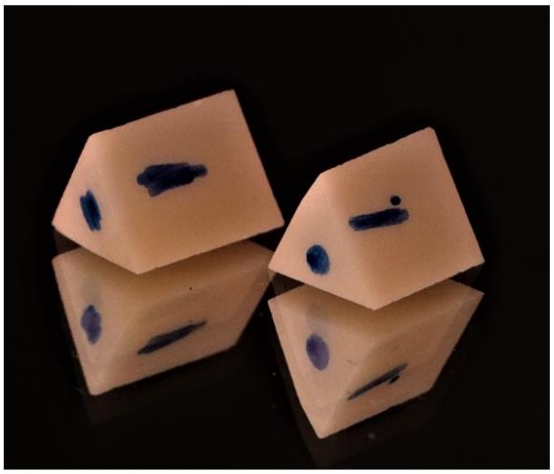

Figure 23: Two halves of the prism specimen marked to allow proper alignment during cementation procedure.

The cementation protocol procedure was carried out using a custom jig (UBC, Faculty of Dentistry, Vancouver, BC, Canada), holding each half of the prism securely by the lid fastened by screws (Fig. 24). The design of the jig allowed the two halves, through a sliding motion, to be brought in contact with the adhesive surfaces adequately aligned.

Figure 24: Alignment of each half of prism specimen in cementation jig.

Once both halves of one sample were secured, placed in each half of the jig, they were bonded using one of the three protocols:

1. Control, with no further treatment and the application of the RCLA
2. MDP, the application of 5 % 10-MDP ethanol primer to both surfaces prior to the application of the RCLA
3. Silane, the application of Bisco Bis-Silane primer to both surfaces prior to the application of the RCLA.

All samples were bonded with RelyX Veneer Cement, the RCLA selected for this study, as the diagram illustrates the adhesive layer for each group Fig. 25.

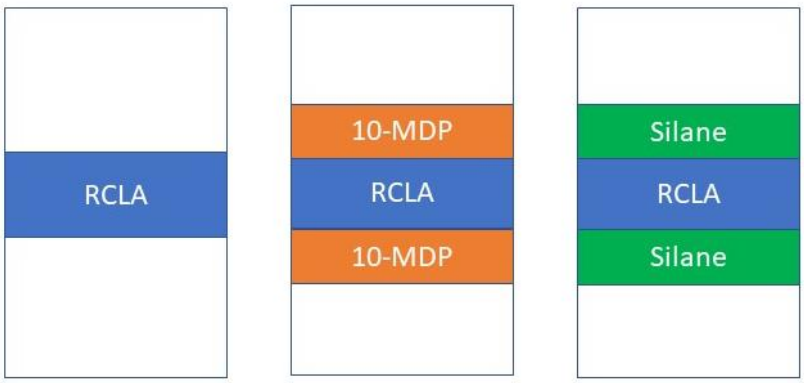

Figure 25: Diagram showing the three groups with different surface treatment: 1) Control, no treatment; 2) MDP, 10 % 10-MDP ethanol primer and 3) Silane, Bisco Bis-Silane. All samples were bonded with an RCLA (3M RelyX Veneer Cement).

The RCLA was applied onto both adhesive surfaces from the syringe, and the two halves were then brought in contact. To ensure a standardized continuous pressure during the setting period of the cement, a weight of 50 g (F = 0.5 N) was placed on the top of the assembly (Fig. 26), and the excess RCLA was removed with a micro-brush. Next, all margins were light-cured for 20 s, followed by additional curing for 20 s after removing the bonded specimens from the holder.

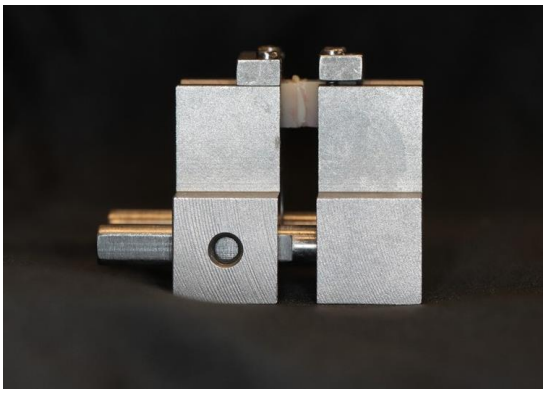

Figure 26: Cementation procedure.

3.2.4 Ageing

Bonded specimens were stored in distilled water at 37 °*C* for 24 hours and 90 days in an Isotemp Incubator Model 630D (Fisher Scientific, Ottawa, Canada) before testing (Fig. 27).

Figure 27: All samples were stored in distilled water at 37 °C for 24 hours before testing. A: Control group; B: MDP, 10 % 10-MDP ethanol primer and C: Silane, Bisco Bis-Silane.

The 24 h specimens were prepared and aged in the first stage of this study. At the end of the 24 h storage, samples belonging to the Control and Silane group were found either debonded in the storage jar or they failed during the manipulation involved in placing the samples in the testing jig. Based on these results, it was decided unnecessary to prepare Control and Silane Group samples for 90 d ageing and testing. Only samples for the MDP Group were prepared, aged and tested at 90 d.

3.2.5 Determination of IK_{1C}

The NTP specimen K_{1C} test was used to determine the IK_{IC}. Each bonded NTP specimen was initially fitted into a custom holder to reproduce the CNSR configuration. The holder consists of two symmetrical parts, each with a loading collar at one end and a triangular prismatic groove at the other, forming the base into which the NTP specimen is placed. The specimen is secured in place by two symmetrical half-disk lids, fastened with screws (Fig. 28).

Figure 28: NTP specimen holder.

The specimen was first placed into one half of the holder, with bonded interface positioned visibly near the edge. Then, under magnification, a sharp razor blade was used to create a ~ 0.1 mm deep crack initiation point along the edge of the NTP specimen. Finally, the second half of the holder was fitted on the other end of the specimen. To ensure a standardized space between the two halves of the holder, a custom mounting jig was used, in which the holder assembly was placed. A 200 µm thick spacer was used to keep the two specimen holder halves apart, replicating the space produced by the cutting blade in the CNSR specimen (Fig. 29).

Figure 29: NTP specimen holder in mounting with spacer.

Prior to testing, a visual inspection under magnification was carried out to ensure the proper position of the NTP specimen into the holder with crack initiation point visible within the bonded interface contained within the space separating the two halves of the holder assembly.

The test assembly was then placed into custom-designed grips connected to a computer-controlled Instron 4301 universal testing machine (UBC, Faculty of Dentistry, Vancouver, BC, Canada), with a 1 kN Instron load cell (Fig. 30). The assembly was loaded in tension at a 0.1 mm/min crosshead speed until crack arrest or crack failure. The load and displacements were monitored and recorded.

Figure 30: NTP specimen loaded for testing.

The maximum load recorded before crack arrest or complete failure was used to calculate the interfacial K_{1C} using the following equation:

$$K_{IC} = \frac{Pmax}{DW^{1/2}} Y^*_{min}$$

Where,

P_{max}: represents maximum load recorded during testing (in N).

D: represents specimen dimeter (12 mm).

W: represents specimen length (10.4 mm).

Y^*_{min}: represents the dimensionless stress intensity factor coefficient, with a value of 28 for the NTP test (97).

3.2.6 Scanning Electron Microscopy (SEM.)

Determining the failure mode at the adhesive interface and topographies of fracture surfaces must be examined under powerful magnification. Possible failure modes of the adhesion interface are illustrated in Fig. 31.

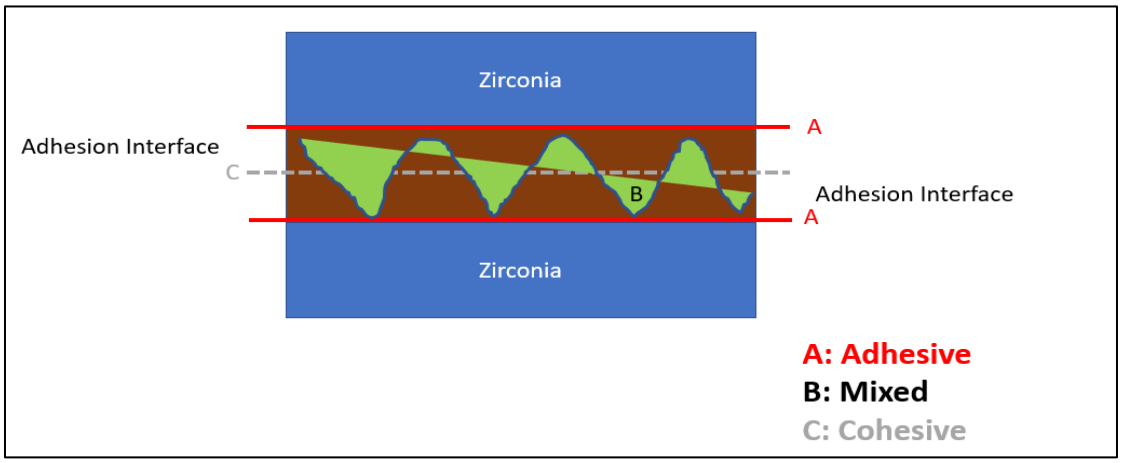

Figure 31: Failure modes of an adhesive interface.

Scanning electron microscopy (SEM) was used to perform the fractographic analysis. Following K_{IC} testing, selected samples closest to the mean IK_{IC} were viewed with an SEM (Hitachi, S-

Figure 32: SEM samples.

3000N; Hitachi, Japan). The specimen halves were labelled and gold-coated with an Edwards S150A sputter coater (Edwards Vacuum, Crawley, UK) (Fig. 32). For each sample, photomicrographs were taken at various magnifications.

3.2.7 Statistical Analysis

The IK_{IC} results obtained for the MDP Group were analyzed with independent samples t-test. The statistical analysis was conducted at (α=0.05), using SPSS (SPSS for Windows, Version 27, Chicago, IL)

Chapter 4: Results

4.1 Interfacial Fracture Toughness (IK_{IC})

The mean and standard deviation IK_{IC} for the MDP groups at the two intervals, along with the results of the independent samples t-tests statistical analysis, are summarized in Table. 6 and presented as box plots in Fig 33.

Table 6: Results of IK_{IC} test (Mean ± SD) in $MPa \cdot m^{1/2}$

Group	***IK*$_{IC}$**	
	24 hours	**90 days**
MDP Group	1.33 ± 0.4^{A}	0.88 ± 0.3^{B}

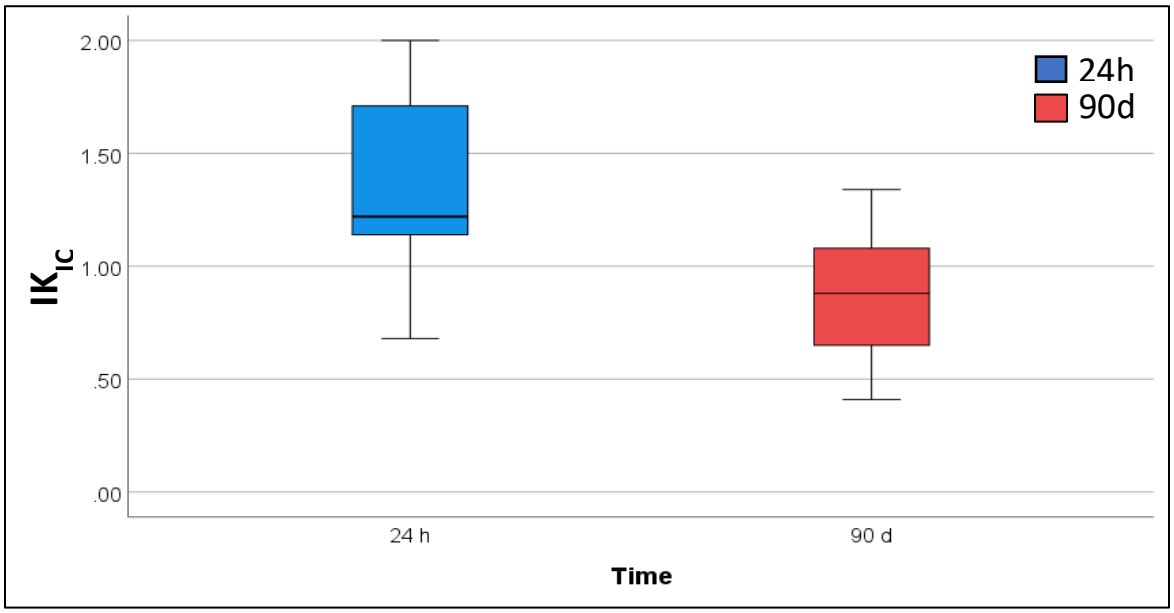

Figure 33: Box plots of the effect of time on IKIC.

Table 7: MDP descriptive statistics.

MDP Group Statistics

	Time	N	Mean	Std. Deviation	Std. Error Mean
KIC	24 h	13	1.33	.40	.11
	90 d	13	.88	.29	.10

Table 8: Independent samples t-tests for MDP group.

		Leven's test for Equality of variances					**t-test for equality of Means**		**95% Confidences interval of the differences**	
		F	**Sig.**	**t**	**df**	**Sig. (2 tailed)**	**Mean differences**	**Std. Error Differences**	**Lower**	**Upper**
IK$_{IC}$	**Equal variances assumed**	**1.03**	**0.32**	**2.93**	**21**	**0.008**	**0.45317**	**0.15455**	**0.13177**	**0.77458**
	Equal variances not assumed			**3.15**	**20.610**	**0.005**	**0.45317**	**0.14387**	**0.15363**	**0.75272**

After storage in 37 °*C* water for 24 h, the only group that could be tested was the MDP group [IK_{IC} = (1.3 ± 0.4) MPa·$m^{1/2}$)]. The samples from the other two groups (Control and Silane) were either de-bonded in water (Silane) or were not able to withstand the manipulation involved in securing the samples in the sample holder (Control) Fig. 34 shows some of the Control and Silane samples after 24 h storage, some of them appearing intact.

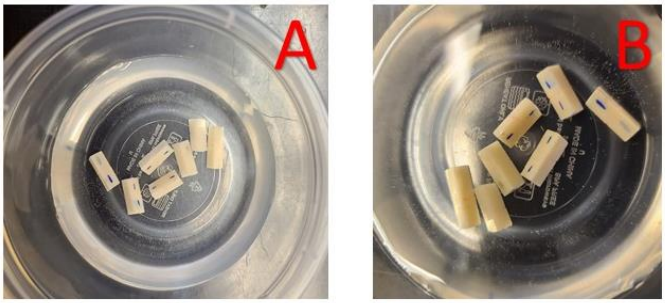

Figure 34: Two groups were intact before testing for 24 h.
A: Control group; B: Silane, Bisco Bis-Silane.

In the 24 h Control and Silane samples, the RCLA was seen either on only one surface of the failed specimen Fig. 35 or as a thin debonded film at the bottom of the storage jar Fig. 36.

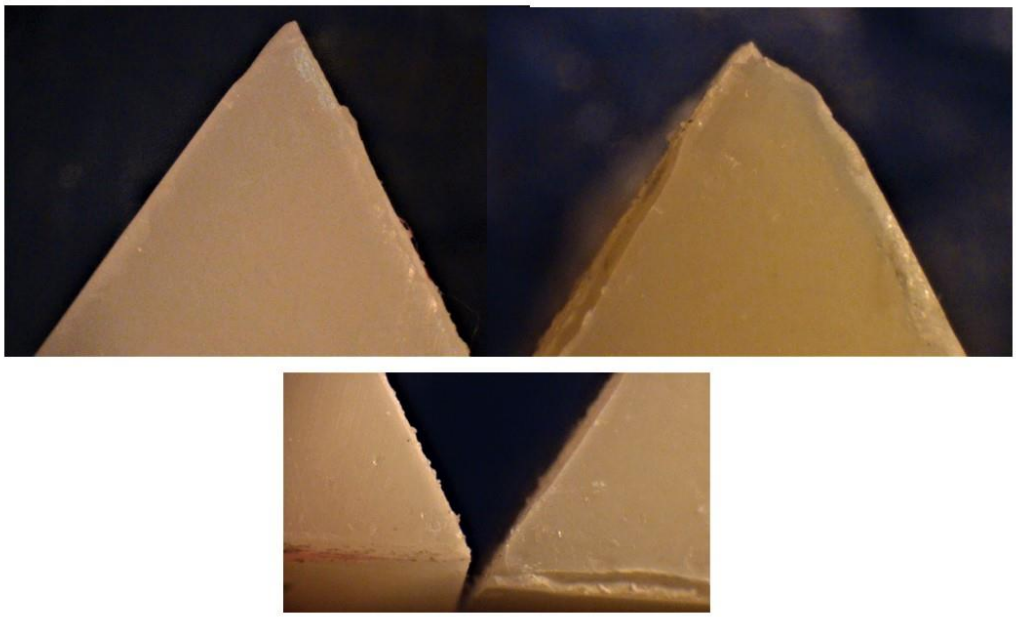

Figure 35: RCLA was seen only on one of the surfaces of failed samples.

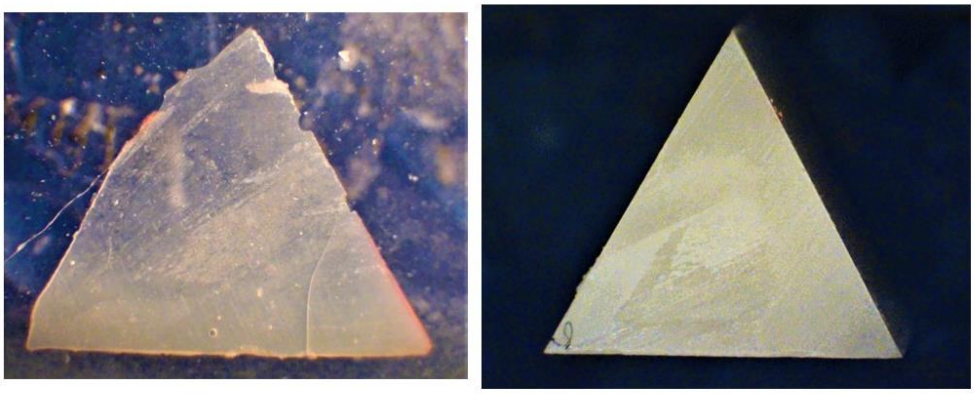

Figure 36: Thin film of RCLA and the clean surface of a debonded sample.

At 90 d storage, the IK_{IC} of the MDP group dropped significantly to (0.88 ± 0.3) MPa·$m^{1/2}$. The results showed that time significantly affected the IK_{IC} between 24 hours and 90 days. A crack-arrested specimen for the MDP group is displayed in Fig 37 and the cohesive failure in RCLA for the MDP group is documented in Fig. 38.

Figure 37: Crack arrest for the MDP group.

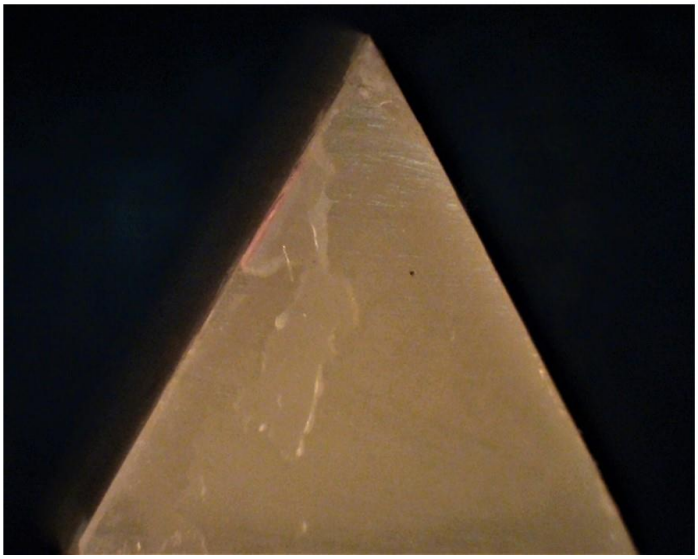

Figure 38: Cohesive failure in RCLA for the MDP group.

The results of this study led to the rejection of the null hypothesis, as the fracture mechanics analysis confirmed the suitability of MDP as a primer for RFZ.

4.2 Resin Composite Luting Agent

The mean and standard deviation K_{IC} for the RCLA at the two intervals, along with the statistical analysis results, are summarized in Table 9 and presented as box plots in Fig. 39.

Table 9: Results of K_{IC} test (Mean ± SD) in $MPa \cdot m^{1/2}$

Group	K_{IC}	
	24 hours	90 days
RCLA Group	0.94 ± 0.12^{A}	0.40 ± 0.12^{B}

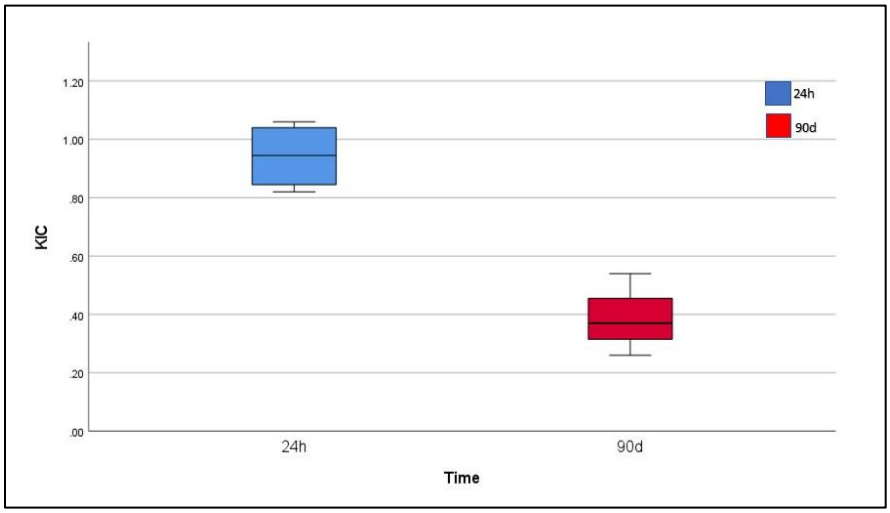

Figure 39: Box plots of the effect of time on RCLA KIC.

After 90 d storage, the K_{IC} of the RCLA dropped significantly, to (0.4 ± 0.12) MPa·m$^{1/2}$.

Table 10: RCLA descriptive statistics.

RCLA Group Statistics

	Time	N	Mean	Std. Deviation	Std. Error Mean
K_{IC}	24h	4	.9425	.11558	.05779
	90d	4	.3850	.11561	.05781

Table 11: Independent samples t-test for RCLA group

		Leven's test for Equality of variances					t-test for equality of Means		95% Confidences interval of the differences	
		F	**Sig.**	**t**	**df**	**Sig. (for 1-tailed & 2 tailed)**	**Mean differences**	**Std. Error Differences**	**Lower**	**Upper**
IK_{IC}	**Equal variances assumed**	**0.265**	**0.265**	**6.820**	**6**	**< 0.001**	**0.55750**	**0.08174**	**0.35749**	**0.75751**
	Equal variances not assumed			**6.820**	**6**	**< 0.001**	**0.55750**	**0.08174**	**0.35749**	**0.75751**

4.3 SEM Characterization

4.3.1 MDP Group

Low and high magnification SEM images of a representative 24 h and 90 d MDP group fractured sample are displayed in Figs. 40 and 41, respectively. At both 24 h and 90 d, fractured surfaces showed surfaces covered with RCLA, indicative of a cohesive failure in the luting agent, suggesting that the adhesion afforded by MDP is stronger than the cohesive strength of the luting agent.

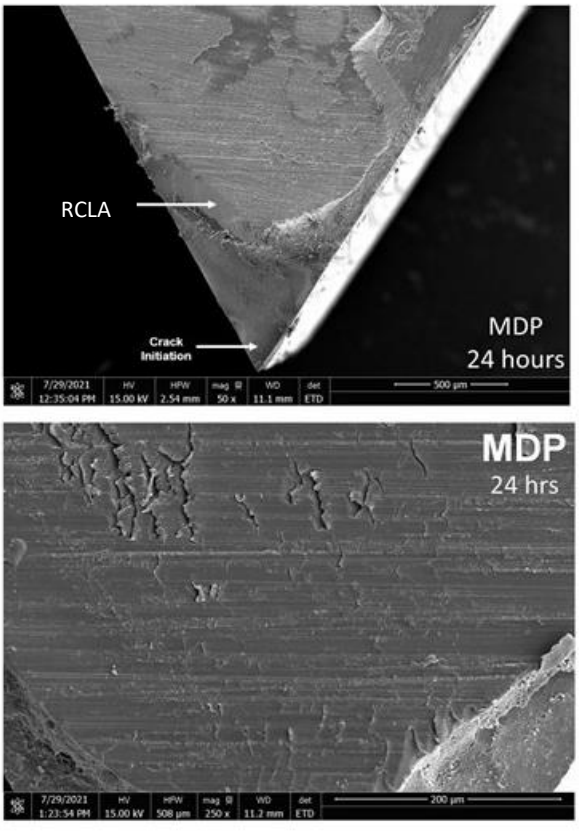

Figure 40: SEM image of 10-MDP at 24 h.

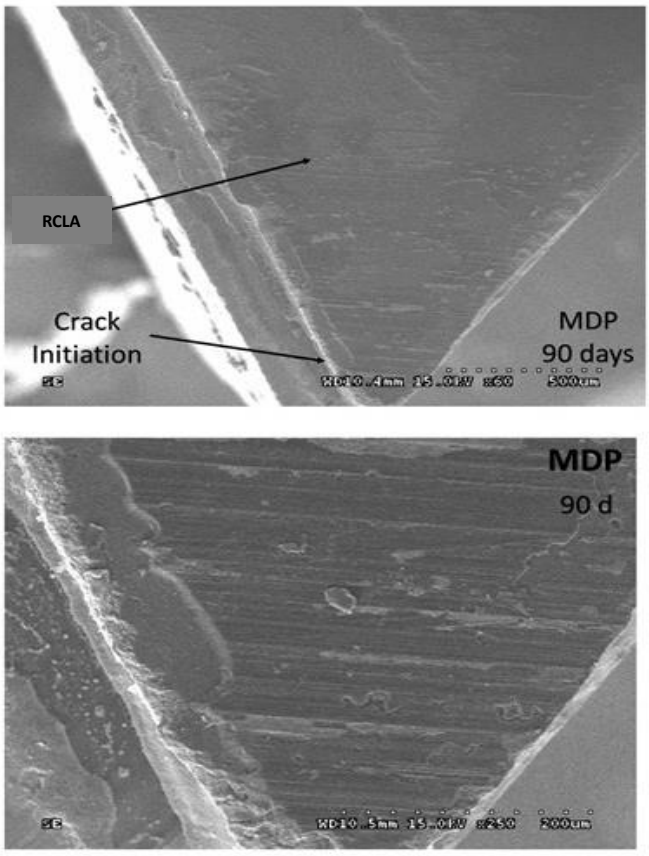

Figure 41: SEM image of 10-MDP at 90 d.

4.3.2 RelyX Veneer Resin Composite Luting Agent

SEM image of a fractured RelyX Veneer NTP specimen is displayed in Fig. 42, showing that fracture was initiated from the induced defect. SEM images of fractured surfaces at 24 h and 90 d (Figs. 43 and 44, respectively) display the surface characteristics/features of the RCLA. These images are similar to those of the fractured MDP samples confirming that in the MDP group fracture occurred cohesively in the RCLA.

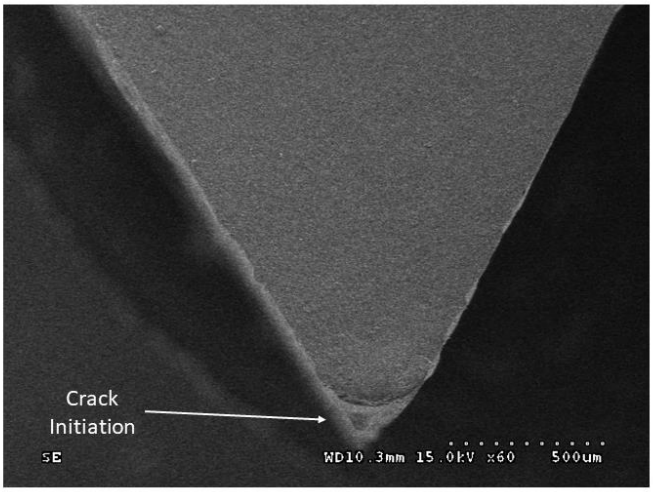

Figure 43: SEM image: Fractured surface/RelyX resin composite luting agent.

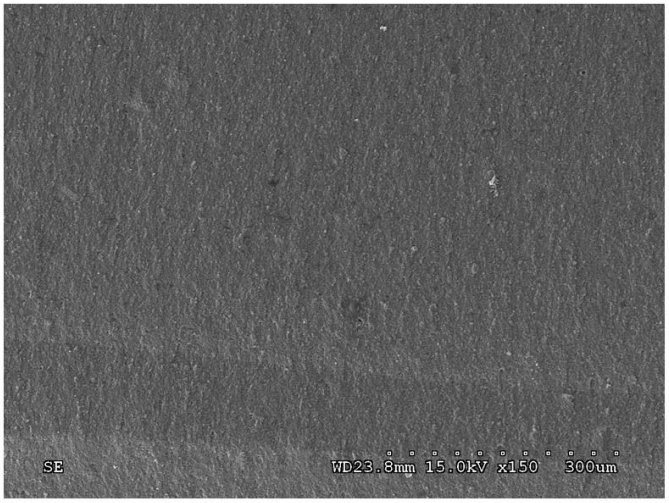

Figure 42: SEM image: Fractured surface (24h)/RelyX resin composite luting agent.

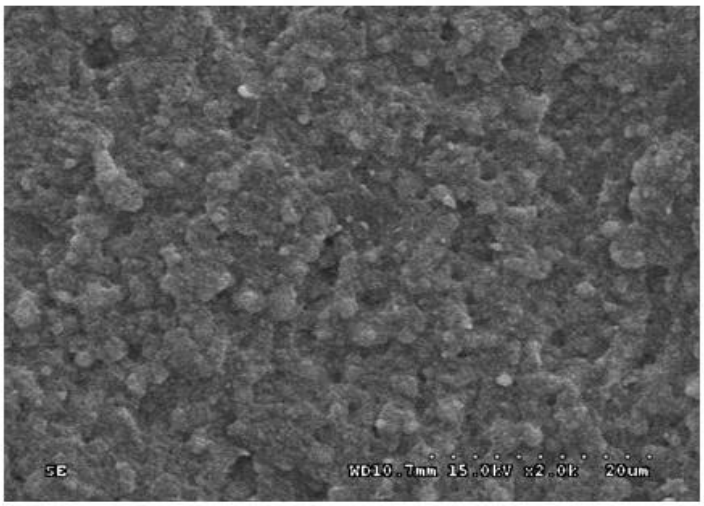

Figure 44: SEM image: Fractured surface (90d)/RelyX resin composite luting agent.

Chapter 5: Discussion

Y-TZP or zirconia restorations have been increasingly used as an alternative to metal-ceramic restorations in daily dental practice, starting as coping and framework materials to be veneered with layering ceramic (porcelain) and later as full-contour monolithic restorations (98). The fast transition of using zirconia was due to its superior mechanical properties, high clinical success, accurate milling fabrication, low wear behavior to antagonist dentition, and fabrications costs (98).

However, as mentioned before, zirconia is a polymorphic material with different temperature-dependent phases. The monoclinic phase is stable from room temperature to 1170 ºC, tetragonal at 1170-2370 *ºC* and cubic over 2370 *ºC*.

Phase transformation from tetragonal to monoclinic is accompanied by a volumetric increase of around 4 % to 5 % (99). Continuous transformation can be prevented by stabilizing the tetragonal phase at room temperature by adding oxides, such as yttria. However, the phase transformation can be triggered if sufficient energy is present at crack tip, which then leads to an increase in volume and the development of compressive stresses, which, in turn, can result in crack closure. This phenomenon, called "transformation toughening", is responsible for the high fracture toughness of tetragonal stabilized zirconia. (100).

The yttria amounts in zirconia broadly define their mechanical and optical properties. Different generations of zirconia can be classified according to their yttria content (mol%). The first generation contained 3 mol% yttria, called 3Y-TZP or conventional zirconia. 3Y-TZP is partially stabilized in the tetragonal phase with the highest fracture toughness (9-10) $MPa.m^{1/2}$ and flexural strength (900-1200) MPa compared to the other generations (101). Therefore, it is the preferred

material for long-span fixed dental prostheses and posterior areas with high occlusal loads (43). However, due to its high opacity and compromised esthetic appearance, 3Y-TZP is predominantly used as a supporting coping and framework structure for bilayer all-ceramic restorations (102).

New generations of zirconia were developed to improve esthetics appearance by increasing the yttria content to 4 mol% and 5 mol% and applying them for full-contour monolithic restorations (103). These generations contain approximately 30 % to 50 % cubic phase particles, making them more translucent and less susceptible to low-temperature degradation (LTD) than conventional 3Y-TZP (104). However, transformation toughening, a crucial factor for superior flexural strength and fracture toughness, does not occur with these compositions. The reduced fracture toughness and flexural strength limit their clinical indication to single unit crown, partial coverage (like inlay or onlay), and short-span fixed dental restorations in areas of limited occlusal load (103).

As with all brittle ceramic materials, resin bonding provides good attachment of indirect ceramic restorations to teeth and increases their resistance to fracture. This is true for silica-based ceramics and lower strength zirconia compositions with limited thickness. However, conventional bonding protocols, using hydrofluoric acid (HF) etching and silane coupling agents applied to glass-ceramics do not provide durable chemical and micromechanical resin bonds to zirconia (104). Different mechanical, chemical, and combined chemical and mechanical surface pre-treatment methods have improved zirconia-resin bonding (105). These consist of airborne-particle abrasion (APA), tribochemical silica airborne-particle abrasion (TBS), low-fusion porcelain application, hot chemical etching solutions, selective infiltration etching (SIE), laser irradiation, plasma spraying, and zirconia ceramic powder coating (106).

Surface pre-treatment methods or techniques aim to improve mechanical and chemical bonds (71). A combination of surface pre-treatment followed by 10-MDP monomer or other phosphate ester monomer-based primers and resin cement has resulted in long-term durable zirconia resin bonds (107). These functional monomers have proven to provide long-lasting chemical bonds to the metal oxides in zirconia (107). Resin bonds to zirconia have been investigated for more than two decades now (102). Classic articles by Kern and coworkers have first verified the effectiveness of APA (Airborne Particle Abrasion) and 10-MDP-containing resin luting agents for long-term zirconia resin bonds (71). Other studies highlighted the importance of a 10-MDP-containing primer, which provides better wettability, especially to the slightly rough CAD/CAM milled surfaces. This primer can also be used with conventional resin composite luting agents.

This bonding protocol to 3Y-TZP consists of three main steps, known as the "APC Zirconia Bonding Concept" (74):

1. Step A: air-particle abrasion with alumina or silica-coated alumina particles.
2. Step P: priming the air-abraded surfaces with 10- MDP or other phosphate-based monomer primer.
3. Step C: cementation with dual or self-cure resin composite luting agent.

Patients' demands for dental restoration with a natural appearance have increased dramatically during the last decades. Translucency is the most important parameter in aesthetics, which is crucial in selecting the restorative material. The new generation of zirconia has intermediate translucency compared to conventional zirconia and lithium disilicate glass-ceramics. Therefore, bonding with this new generation zirconia is crucial for long-term clinical success. This in-vitro

study aimed to investigate the effect of 10-MDP on the adherence of a RCLA to RFZ by determining the IK_{IC} and comparing the results with other studies to assess its suitability.

In this study, the 10-MDP was used without any prior surface treatment, such as air abrasive or other techniques. The 24 h IK_{IC} of the MDP group was (1.34±0.40) MPa·$m^{1/2}$ and crack propagation occurred cohesively through the RCLA. Following the 90 d storage, the IK_{IC} of the MDP group dropped significantly to (0.88 ± 0.3) MPa·$m^{1/2}$, but crack propagation occurred cohesively through the RCLA. These results showed that the 10-MDP mediated adherence to RFZ was stronger than the cohesive strength of the RCLA at both 24 h and 90 d.

The results were compared with those of other studies that used different pre-treatment and non-treatment surfaces. However, no studies comparing the IK_{IC} of RFZ after application of 10-MDP are available in the literature. Mehari et al. (108) compared the effect of three surface treatments on the shear bond strength of 10-MDP-mediated bonding to new generation zirconia (4Y-TZP and 5Y-TZP): 1) without surface pre-treatment; 2) APA with alumina 50 µm at 2 bar pressure; and 3) 80 µm glass bead. The samples were stored for 24 h in distilled water and thermocycled for 2500 cycles before the shear test. The bond strength for the non-treated zirconia surface showed reduced bond values [6.4 ± 1.4 MPa] compared to the APA treatment [12.9 ± 3.4 MPa] . The failure modes were mainly adhesive and mixed failure.

The study by Franco-Tabares et al. (99) used both new generations zirconia without surface pre-treatment using Panavia F 2.0 (Kuraray, Tokyo, Japan) as a resin cement with 10-MDP as primer. After storage in distilled water for 24 h, the shear bond strength to 4Y-TZP was (4.81 ± 1.2) MPa, while to 5Y-TZP was (6.01 ± 1.2) MPa. However, they did not characterize the mode of the failure.

Yogawa et al. (109), in their study, set out to evaluate the effect of priming agents and artificial ageing with thermocycling on shear bond strengths of two resin-based luting agents to a translucent zirconia material. The result showed that the groups with 10-MDP primer had higher bond strength (47.8 ± 3.6) MPa l while the groups that did not apply the primer 10-MDP had less shear bond strength (32.4 ± 2.2) MPa l. In their conclusion, the application of priming agents containing hydrophobic phosphate monomer 10-MDP lead to durable bond strengths of resin-based luting agents to a translucent zirconia material.

Ruales-Carrera et al. (110) aimed to evaluate the adhesive behaviour of conventional and high-translucent zirconia after surface conditioning and hydrothermal ageing using the shear bond strength. Conventional and high-translucent zirconia specimens were divided into six groups: without surface treatment, airborne particle abrasion with 50-μm Al_2O_3 sized particles, and tribochemical treatment with 30-μm silica modified Al_2O_3 sized particles. Zirconia specimens were treated using a 10-MDP-containing universal adhesive and bonded to two resins blocks with adhesive luting cement. The roughness of the groups that used airborne particle abrasion with 50-μm Al_2O_3 sized particles was statistically higher. Mixed failure was most frequent for the mechanically treated groups, while no cohesive failures were observed. In his conclusion found the lower values of bond strength were obtained for treated high-translucent zirconia groups when compared to conventional zirconia counterparts. Mechanical surface treatment significantly improved the bond strength to conventional and high-translucent zirconia associated with the use of universal adhesives containing 10-MDP could provide a durable bonding to conventional and high-translucent zirconia.

Monterio et al. (111) focused on examining the effect of different surface treatments on the retention between zirconia crowns and tooth structure after in vitro ageing. Their study used human

third molars that received crown preparations and manufactured CAD/CAM zirconia crowns. Specimens were divided into two groups: no ageing (control group) and ageing (experimental group). The control group was bonded with universal adhesive. Aged specimens were divided into three subgroups according to surface treatment: Control, no abrasion; Alumina, alumina abrasion; Silica, tribochemical silica coating. All three groups were bonded with universal adhesive. The crowns were cemented with dual-cure resin cement. Tensile tests were used to assess the retention strength values. The lowest value was for the control group with universal adhesive (0.8 ± 0.3) MPa, and the failure mode was only adhesive. The long-term retention of translucent zirconia crowns to tooth structure using phosphate-based materials was improved by utilizing mechanical surface treatments such as alumina blasting and tribochemical silica coating.

Experimental designs and testing setups varied significantly between studies. Several testing methods (i.e., shear, tensile and micro-tensile) were applied to measure and compare bond strength of resin cement to new zirconia generations, with the shear-bond strength test being the most common. This might be due to its user-friendliness, simple specimen preparation, clear test protocol, and fast results (112). However, the shear test has been criticized for developing non-homogenous stress distributions over the ceramic interface. Its fracture pattern may cause cohesive failures, leading to inaccurate interpretations of the results (113) and a failure to simulate clinical conditions. Tensile tests, on the other hand, provide more homogenous stress distribution. Fracture patterns occur within the adhesive interface, which seems more appropriate for evaluating bond strength values (114). Micro-tensile tests are claimed to be the most suitable method (115). They offer better distribution of stresses and more sensitive analysis. However, a significant limitation is the demanding and technique-sensitive specimen preparation.

On the other hand, the microscopic analysis of the failure mode type is necessary to understand the obtained bond strength values (106). In addition, ageing plays an essential role in evaluating the effects of intraoral conditions in terms of temperature changes in a wet environment.

Some studies suggest that mechanical surface pre-treatment and the use of 10-MDP or another phosphate monomer-based primer or resin cement is recommended for new zirconia generations. However, most of the studies did not use clinically relevant specimen geometries, and flat discs or cylinders fail to reproduce actual stresses at the zirconia-tooth interface (116). There is also little information on the influence of the tested bonding protocols on the flexural strength and other physical properties of new zirconia generations.

Chapter 6: Conclusions

Within the limitations of this study, the results obtained suggests that:

1. 10-Methacryloyloxdecyl-dihydrogen phosphate (10-MDP) is able mediate adhesion to rapid fired, highly translucent zirconia
2. The interfacial fracture toughness of the 10-MDP-mediated adhesive bond dropped during 90 d ageing in 37 °C water but was superior to the cohesive strength of the resin composite luting agent
3. Results of clinical trials will ultimately validate these findings.

References

1. Kelly JR, Nishimura I, Campbell SD. Ceramics in dentistry: Historical roots and current perspectives. J Prosthet Dent. 1996;75(1):18–32.

2. Heffernan MJ. Relative translucency of six all-ceramic systems. Part II: Core and veneer materials. J Prosthet Dent. 2002;88(1):10–5.

3. Fischer H, Marx R. Fracture toughness of dental ceramics: Comparison of bending and indentation method. Dent Mater. 2002;18(1):12–9.

4. Denry I, Holloway JA. Ceramics for dental applications: A review. Materials (Basel). 2010;3(1):351–68.

5. Valderhaug J. A 15-year clinical evaluation of fixed prosthodontics. Acta Odontol Scand. 1991;49(1):35–40.

6. Warreth A, Elkareimi Y. All-ceramic restorations: A review of the literature. Saudi Dent J . 2020;32(8):365–72. https://doi.org/10.1016/j.sdentj.2020.05.004

7. Lopes SC, Pagnano VO, De Almeida Rollo JMD, Leal MB, Bezzon OL. Correlation between metal-ceramic bond strength and coefficient of linear thermal expansion difference. J Appl Oral Sci. 2009;17(2):122–8.

8. Peampring C, Sanohkan S. All-ceramic systems in Esthetic Dentistry: A review. M Dent J. 2014;34:82-90..

9. Anusavice KJ, Shen C RH. Phillips' science of dental materials. 12th ed., Elsevier Health Sciences; 2013.

10. McLaren EA, Whiteman YY. Ceramics: rationale for material selection. Compend Contin Educ Dent. 2010;31(9):666-668.

11. Beuer F, Schweiger J, Eichberger M, Kappert HF, Gernet W, Edelhoff D. High-strength CAD/CAM-fabricated veneering material sintered to zirconia copings - A new fabrication mode for all-ceramic restorations. Dent Mater. 2009;25(1):121–8.

12. Holden JE, Goldstein GR, Hittelman EL, Clark EA. Comparison of the marginal fit of pressable ceramic to metal ceramic restorations. J Prosthodont. 2009;18(8):645–8.

13. Rekow ED, Silva NRFA, Coelho PG, Zhang Y, Guess P, Thompson VP. Performance of dental ceramics: Challenges for improvements. J Dent Res. 2011;90(8):937–52.

14. Hamza TA, Sherif RM. Fracture Resistance of Monolithic Glass-Ceramics Versus Bilayered Zirconia-Based Restorations. J Prosthodont. 2019;28(1):e259–64.

15. Powers J, Wataha J. Dental Materials : Foundations and Applications. 11th ed. Mosby; 2017.

16. Kelly JR, Benetti P. Ceramic materials in dentistry: Historical evolution and current practice. Aust Dent J. 2011;56(SUPPL. 1):84–96.

17. Fradeani M, Redemagni M. An 11-year clinical evaluation of leucite-reinforced glass-ceramic crowns: a retrospective study. Quintessence Int . 2002;33(7):503–10. http://www.ncbi.nlm.nih.gov/pubmed/12165985

18. Wolfart S, Eschbach S, Scherrer S, Kern M. Clinical outcome of three-unit lithium-disilicate glass-ceramic fixed dental prostheses: Up to 8 years results. Dent Mater. 2009;25(9):63–71.

19. Guess PC, Zhang Y, Thompson VP. Effect of veneering techniques on damage and reliability of Y-TZP trilayers. Eur J Esthet Dent. 2009;4 3:262–76.

20. Lekesiz H. Reliability estimation for single-unit ceramic crown restorations. J Dent Res. 2014;93(9):923–8.

21. Aboushelib MN, De Jager N, Kleverlaan CJ, Feilzer AJ. Microtensile bond strength of different components of core veneered all-ceramic restorations. Dent Mater. 2005;21(10):984–91.

22. Shenoy A, Shenoy N. Dental ceramics: An update. J Conserv Dent. 2010;13(4):195-203.

23. Guazzato M, Albakry M, Ringer SP, Swain M V. Strength, fracture toughness and microstructure of a selection of all-ceramic materials. Part I. Pressable and alumina glass-infiltrated ceramics. Dent Mater. 2004;20(5):441–8.

24. Moshiri Z. Zirconia : An Up-to-date Literature Review. Avicenna J Dent Res. 2013;4(1):1–15.

25. Chevalier J, Gremillard L. Zirconia as a biomaterial. Compr Biomater. 2011;1:95–108.

26. Covacci V, Bruzzese N, Maccauro G, Andreassi C, Ricci GA, Piconi C, et al. In vitro evaluation of the mutagenic and carcinogenic power of high purity zirconia ceramic. Biomaterials. 1999;20(4):371–6.

27. Brodbeck URS. The ZiReal Post: A New Ceramic Implant Abutment. J Esthet Restor Dent. 2003;15(1):10–24.

28. Walker PD. “CAD-on” interfaces - a fracture mechanics characterization . 2017.

https://open.library.ubc.ca/collections/24/items/1.0354411

29. Piconi C, Maccauro G. Zirconia as a ceramic biomaterial. Biomaterials. 1999;20(1):1–25.

30. Lughi V, Sergo V. Low temperature degradation -aging- of zirconia: A critical review of the relevant aspects in dentistry. Dent Mater . 2010;26(8):807–20. http://dx.doi.org/10.1016/j.dental.2010.04.006

31. Vagkopoulou T, Koutayas SO, Koidis P, Strub JR. Zirconia in dentistry: Part 1. Discovering the nature of an upcoming bioceramic. Eur J Esthet Dent. 2009;4(2):130–51.

32. Kosmac T, Oblak C, Jevnikar P, Funduk N, Marion L. Strength and reliability of surface treated Y-TZP dental ceramics. J Biomed Mater Res. 2000;53(4):304–13.

33. Olsson K-G, Fürst B, Andersson B, Carlsson GE. A long-term retrospective and clinical follow-up study of In-Ceram Alumina FPDs. Int J Prosthodont. 2003;16(2):150–6.

34. Denry I, Kelly JR. State of the art of zirconia for dental applications. Dent Mater. 2008;24(3):299–307.

35. Guazzato M, Albakry M, Swain M V., Ringer SP. Microstructure of alumina- and alumina/zirconia-glass infiltrated dental ceramics. Key Eng Mater. 2003;240–242:879–82.

36. Sundh A, Cam CAD. Fracture resistance of all-ceramic zirconia bridges with differing phase stabilizers and quality of sintering. 2005;2:778–84.

37. Hannink RHJ, Kelly PM MB. Transformation Toughening in Zirconia-Containing Ceramics. J Am Ceram Soc. 2000;83(3):461–87.

38. He Y, Winnubst L, Burggraaf AJ, Verweij H, van der Varst PGTh, de With B. Influence of Porosity on Friction and Wear of Tetrgonal Zirconia Polycrystal. J Am Ceram Soc. 1997;80:377–80.

39. Mazaheri M, Simchi A, Golestani-Fard F. Densification and grain growth of nanocrystalline 3Y-TZP during two-step sintering. J Eur Ceram Soc. 2008;28(15):2933–9.

40. Zarone F, Russo S, Sorrentino R. From porcelain-fused-to-metal to zirconia: Clinical and experimental considerations. Dent Mater. 2011;27(1):83–96. http://dx.doi.org/10.1016/j.dental.2010.10.024

41. Chevalier J, Deville S, Münch E, Jullian R, Lair F. Critical effect of cubic phase on aging in 3 mol% yttria-stabilized zirconia ceramics for hip replacement prosthesis. Biomaterials. 2004;25(24):5539–45.

42. Cottom BA, Mayo MJ. Fracture toughness of nanocrystalline ZrO_2-3mol% Y_2O_3 determined by vickers indentation. Scr Mater. 1996;34(5):809–14.

43. Miyazaki T, Nakamura T, Matsumura H, Ban S, Kobayashi T. Current status of zirconia restoration. J Prosthodont Res. 2013;57(4):236–61. http://dx.doi.org/10.1016/j.jpor.2013.09.001

44. Øilo M, Kvam K, Gjerdet NR. Load at fracture of monolithic and bilayered zirconia crowns with and without a cervical zirconia collar. J Prosthet Dent. 2016;115(5):630–6. http://dx.doi.org/10.1016/j.prosdent.2015.11.017

45. Choi JW, Kim SY, Bae JH, Bae E Bin, Huh JB. In vitro study of the fracture resistance of

monolithic lithium disilicate, monolithic zirconia, and lithium disilicate pressed on zirconia for three-unit fixed dental prostheses. J Adv Prosthodont. 2017;9(4):244–51.

46. Sailer I, Balmer M, Hüsler J, Hämmerle CHF, Känel S, Thoma DS. 10-year randomized trial (RCT) of zirconia-ceramic and metal-ceramic fixed dental prostheses. J Dent. 2018;76(May):32–9. https://doi.org/10.1016/j.jdent.2018.05.015

47. Al-Amleh B, Lyons K, Swain M. Clinical trials in zirconia: a systematic review. J Oral Rehabil. 2010;37(8):641–52.

48. Chaar MS, Passia N, Kern M. Ten-year clinical outcome of three-unit posterior FDPs made from a glass-infiltrated zirconia reinforced alumina ceramic (In-Ceram Zirconia). J Dent. 2015;43(5):512–7. http://dx.doi.org/10.1016/j.jdent.2015.02.016

49. Rinke S, Gersdorff N, Lange K, Roediger M. Prospective evaluation of zirconia posterior fixed partial dentures: 7-year clinical results. Int J Prosthodont. 2013;26(2):164–71.

50. Zhang Y. Making yttria-stabilized tetragonal zirconia translucent. Dent Mater. 2014;30(10):1195–203. http://dx.doi.org/10.1016/j.dental.2014.08.375

51. Zhang F, Inokoshi M, Batuk M, Hadermann J, Naert I, Van Meerbeek B, et al. Strength, toughness and aging stability of highly-translucent Y-TZP ceramics for dental restorations. Dent Mater. 2016;32(12):e327–37. http://dx.doi.org/10.1016/j.dental.2016.09.025

52. Kolakarnprasert N, Kaizer MR, Kim DK, Zhang Y. New multi-layered zirconias: Composition, microstructure and translucency. Dent Mater. 2019;35(5):797–806. https://doi.org/10.1016/j.dental.2019.02.017

53. Zhang Y, Lawn BR. Novel Zirconia Materials in Dentistry. J Dent Res. 2018;97(2):140–7.

54. Kwon SJ, Lawson NC, McLaren EE, Nejat AH, Burgess JO. Comparison of the mechanical properties of translucent zirconia and lithium disilicate. J Prosthet Dent. 2018;120(1):132–7. https://doi.org/10.1016/j.prosdent.2017.08.004

55. Lawson NC, Maharishi A. Strength and translucency of zirconia after high-speed sintering. J Esthet Restor Dent. 2020;32(2):219–25.

56. Abdulla M, Ali H, Jamel R. CAD-CAM Technology: A literature review. Al-Rafidain Dent J. 2020;20(1):95–113.

57. Grant GT, Campbell SD, Masri RM, Andersen MR. Glossary of Digital Dental Terms: American College of Prosthodontists. J Prosthodont. 2016;25:S2–9.

58. A. Sadan, M. B. Blatz and BL. Clinical considerations for densely sintered alumina and zirconia restorations: Part 1. Int J Perio Rest Dent. 2005;25(3):213–9.

59. Mörmann WH. The evolution of the CEREC system. J Am Dent Assoc. 2006;137(9 SUPPL.):7–13.

60. Lucsanszky IJR, Ruse ND. Fracture Toughness, Flexural Strength, and Flexural Modulus of New CAD/CAM Resin Composite Blocks. J Prosthodont. 2020;29(1):34–41.

61. Breschi L, Mazzoni A, Ruggeri A, Cadenaro M, Di Lenarda R, De Stefano Dorigo E. Dental adhesion review: Aging and stability of the bonded interface. Dent Mater. 2008;24(1):90–101.

62. Zhao Z, Wang Q, Zhao J, Zhao B, Ma Z, Zhang C. Adhesion of Teeth. Front Mater.

2021;7(January):1–11.

63. Buonocore MG. A Simple Method of Increasing the Adhesion of Acrylic Filling Materials to Enamel Surfaces. J Dent Res. 1955;34(6):849–53. https://doi.org/10.1177/00220345550340060801

64. Comino-Garayoa R, Peláez J, Tobar C, Rodríguez V, Suárez MJ. Adhesion to zirconia: A systematic review of surface pretreatments and resin cements. Materials (Basel). 2021;14(11):2751.

65. Breschi L, Mazzoni A, De Stefano Dorigo E, Ferrari M. Adhesion to intraradicular dentin: A review. J Adhes Sci Technol. 2009;23(7–8):1053–83.

66. Van Meerbeek B, De Munck J, Yoshida Y, Inoue S, Vargas M, Vijay P et al. Buonocore memorial lecture. Adhesion to enamel and dentin: current status and future challenges. Oper Dent. 2003;28(3):215–35.

67. Carvalho RM, Chersoni S, Frankenberger R, Pashley DH, Prati C, Tay FR. A challenge to the conventional wisdom that simultaneous etching and resin infiltration always occurs in self-etch adhesives. Biomaterials. 2005;26(9):1035–42.

68. Da Rosa WLDO, Piva E, Da Silva AF. Bond strength of universal adhesives: A systematic review and meta-analysis. J Dent. 2015;43(7):765–76. http://dx.doi.org/10.1016/j.jdent.2015.04.003

69. Flamant Q, Anglada M. Hydrofluoric acid etching of dental zirconia. Part 2: Effect on flexural strength and ageing behavior. J Eur Ceram Soc. 2016;36(1):135–45.

http://dx.doi.org/10.1016/j.jeurceramsoc.2015.09.022

70. Thompson JY, Stoner BR, Piascik JR, Smith R. Adhesion/cementation to zirconia and other non-silicate ceramics: Where are we now? Dent Mater. 2011;27(1):71–82. http://dx.doi.org/10.1016/j.dental.2010.10.022

71. Kern M, Wegner SM. Bonding to zirconia ceramic: Adhesion methods and their durability. Dent Mater. 1998;14(1):64–71.

72. Kern M, Thompson VP. Bonding to glass infiltrated alumina ceramic: Adhesive methods and their durability. J Prosthet Dent. 1995;73(3):240–9.

73. Wegner, S M; Kern M. Long-term resin bond strength to zirconia ceramic. J Adhes Dent. 2000;2(2):139-147.

74. Blatz MB, Alvarez M, Sawyer K, Brindis M. How to Bond Zirconia: The APC Concept. Compend Contin Educ Dent. 2016;37(9):611–8.

75. Russo DS, Cinelli F, Sarti C, Giachetti L. Adhesion to zirconia: A systematic review of current conditioning methods and bonding materials. Dent J. 2019;7(3):192-201.

76. Yenisey M, Dede DÖ, Rona N. Effect of surface treatments on the bond strength between resin cement and differently sintered zirconium-oxide ceramics. J Prosthodont Res. 2016;60(1):36–46.

77. Ozcan M. Air abrasion of zirconia resin-bonded fixed dental prostheses prior to adhesive cementation: why and how? J Adhes Dent. 2013;15(4):394. http://www.ncbi.nlm.nih.gov/pubmed/23926592

78. Tsuchimoto Y, Yoshida Y, Mine A, Nakamura M, Nishiyama N, Van Meerbeek B, et al. Effect of 4-MET- and 10-MDP-based primers on resin bonding to titanium. Dent Mater J. 2006;25(1):120–4.

79. Chen Y, Lu Z, Qian M, Zhang H, Chen C, Xie H, et al. Chemical affinity of 10-methacryloyloxydecyl dihydrogen phosphate to dental zirconia: Effects of molecular structure and solvents. Dent Mater. 2017;33(12):e415–27. http://dx.doi.org/10.1016/j.dental.2017.09.013

80. De Souza G, Hennig D, Aggarwal A, Tam LE. The use of MDP-based materials for bonding to zirconia. J Prosthet Dent. 2014;112(4):895–902. http://dx.doi.org/10.1016/j.prosdent.2014.01.016

81. Yoshida K, Tsuo Y AM. Bonding of Dual-cured Resin Cement to Zirconia Ceramic Using Phosphate Acid Ester Monomer and Zirconate Coupler. J Biomed Mater Res B Appl Biomater. 2006;77B(1):28–33.

82. Brandt WC, Schneider LFJ, Frollini E, Correr-Sobrinho L, Sinhoreti MAC. Effect of different photo-initiators and light curing units on degree of conversion of composites. Braz Oral Res. 2010;24(3):263–70.

83. Krämer N, Lohbauer U, Frankenberger R. Adhesive luting of indirect restorations. Am J Dent. 2000;13(Spec No):60D-76D.

84. El-Badrawy WA, El-Mowafy OM. Chemical versus dual curing of resin inlay cements. J Prosthet Dent. 1995;73(6):515–24.

85. Hasegawa EA, Boyer DB, Chan DCN. Hardening of dual-cured cements under composite resin inlays. J Prosthet Dent. 1991;66(2):187–92.

86. Braga RR, Meira JBC, Boaro LCC, Xavier TA. Adhesion to tooth structure: A critical review of "macro" test methods. Dent Mater. 2010;26(2):38–49.

87. Van Meerbeek B, Peumans M, Poitevin A, Mine A, Van Ende A, Neves A, et al. Relationship between bond-strength tests and clinical outcomes. Dent Mater. 2010;26(2):100–21.

88. Van Noort R, Noroozi S, Howard IC, Cardew G. A critique of bond strength measurements. J Dent. 1989;17(2):61–7.

89. Della Bona A, Van Noort R. Shear vs. Tensile Bond Strength of Resin Composite Bonded to Ceramic. J Dent Res. 1995;74(9):1591–6.

90. Medical T, Paulo S. 1-S2.0-0109564194900671-Main. Dent Mater. 1994;10:236–40.

91. Armstrong S, Geraldeli S, Maia R, Raposo LHA, Soares CJ, Yamagawa J. Adhesion to tooth structure: A critical review of "micro" bond strength test methods. Dent Mater. 2010;26(2):50–62.

92. Yin L, Nakanishi Y, Alao AR, Song XF, Abduo J, Zhang Y. A Review of Engineered Zirconia Surfaces in Biomedical Applications. Procedia CIRP. 2017;65:284–90. http://dx.doi.org/10.1016/j.procir.2017.04.057

93. Sudsangiam S, van Noort R. Do dentin bond strength tests serve a useful purpose? J Adhes Dent . 1999;1(1):57–67. http://www.ncbi.nlm.nih.gov/pubmed/11725686

94. Scherrer SS, Cesar PF, Swain M V. Direct comparison of the bond strength results of the different test methods: A critical literature review. Dent Mater. 2010;26(2).

95. Soderholm KJ. Review of the fracture toughness approach. Dent Mater. 2010;26(2):63–77.

96. Sakaguchi RL, Powers JM. Craig ’s Restorative Dental Materials. 2012. 340, 342–343, 95,97 p.

97. Ruse ND, Troczynski T, MacEntee MI, Feduik D. Novel fracture toughness test using a notchless triangular prism (NTP) specimen. J Biomed Mater Res. 1996;31(4):457–63.

98. Alammar A, Blatz MB. The resin bond to high-translucent zirconia—A systematic review. J Esthet Restor Dent. 2022;34:1–19.

99. Kelly JR, Denry I. Stabilized zirconia as a structural ceramic: An overview. Dent Mater. 2008;24(3):289–98.

100. Hannink RHJ, Kelly PM, Muddle BC. Transformation toughening in zirconia-containing ceramics. J Am Ceram Soc. 2000;83(3):461–87.

101. Jansen JU, Lümkemann N, Letz I, Pfefferle R, Sener B, Stawarczyk B. Impact of high-speed sintering on translucency, phase content, grain sizes, and flexural strength of 3Y-TZP and 4Y-TZP zirconia materials. J Prosthet Dent. 2019;122(4):396–403. https://doi.org/10.1016/j.prosdent.2019.02.005

102. Sailer I, Balmer M, Hüsler J, Hämmerle C, Känel S, Thoma D. Comparison of Fixed Dental Prostheses with Zirconia and Metal Frameworks: Five-Year Results of a Randomized Controlled Clinical Trial. Int J Prosthodont. 2017;30(5):426–8.

103. Güth J-F, Stawarczyk B, Edelhoff D, Liebermann A. Zirconia and its novel compositions: What do clinicians need to know? Quintessence Int. 2019;50(7):512–20.

104. Jerman E, Lümkemann N, Eichberger M, Zoller C, Nothelfer S, Kienle A, et al. Evaluation of translucency, Marten's hardness, biaxial flexural strength and fracture toughness of 3Y-TZP, 4Y-TZP and 5Y-TZP materials. Dent Mater. 2021;37(2):212–22. https://doi.org/10.1016/j.dental.2020.11.007

105. Blatz MB, Vonderheide M, Conejo J. The Effect of Resin Bonding on Long-Term Success of High-Strength Ceramics. J Dent Res. 2018;97(2):132–9.

106. Papia E, Larsson C, Du Toit M, Von Steyern PV. Bonding between oxide ceramics and adhesive cement systems: A systematic review. J Biomed Mater Res - Part B Appl Biomater. 2014;102(2):395–413.

107. Aboushelib MN, Matinlinna JP, Salameh Z, Ounsi H. Innovations in bonding to zirconia-based materials: Part I. Dent Mater. 2008;24(9):1268–72.

108. Mehari K, Parke AS, Gallardo FF, Vandewalle KS. Assessing the effects of air abrasion with aluminum oxide or glass beads to zirconia on the bond strength of cement. J Contemp Dent Pract. 2020;21(7):713–7.

109. Yagawa S, Komine F, Fushiki R, Kubochi K, Kimura F, Matsumura H. Effect of priming agents on shear bond strengths of resin-based luting agents to a translucent zirconia material. J Prosthodont Res. 2018;62(2):204–9. http://dx.doi.org/10.1016/j.jpor.2017.08.011

110. Ruales-Carrera E, Cesar PF, Henriques B, Fredel MC, Özcan M, Volpato CAM. Adhesion behavior of conventional and high-translucent zirconia: Effect of surface conditioning methods and aging using an experimental methodology. J Esthet Restor Dent. 2019;31(4):388–97.

111. Monteiro RV, dos Santos DM, Bernardon JK, De Souza GM. Effect of surface treatment on the retention of zirconia crowns to tooth structure after aging. J Esthet Restor Dent. 2020;32(7):699–706.

112. Oilo G. Bond strength testing--what does it mean? Int Dent J. 1993 Oct;43(5):492–8.

113. Blatz MB, Sadan A, Kern M. Resin-ceramic bonding: A review of the literature. J Prosthet Dent. 2003;89(3):268–74.

114. Nicholls JI. Tensile bond of resin cements to porcelain veneers. J Prosthet Dent. 1988;60(4):443–7.

115. Özcan M, Bernasconi M. Adhesion to zirconia used for dental restorations: a systematic review and meta-analysis. J Adhes Dent. 2015 Feb;17(1):7–26.

116. Komine F, Tomic M, Gerds T, Strub JR. Influence of different adhesive resin cements on the fracture strength of aluminum oxide ceramic posterior crowns. J Prosthet Dent. 2004;92(4):359–64.